

Functionalization of Lignin Nanoparticles

Ana Rita Mendes Alves

Thesis to obtain the Master of Science Degree in

Chemical Engineering

Supervisors:

Professor Anton Friedl (TU Wien)

Professor Ana Clara Lopes Marques (IST)

Examination Committee:

Chairperson: Henrique Matos

Supervisor: Anton Friedl (TU Wien), Ana Clara Lopes Marques (IST)

Member of the Committee: Rui Galhano

October 2019

Declaration

I declare that this document is an original work of my own authorship and that it fulfils all the requirements of the Code of Conduct and Good Practices of the Universidade de Lisboa.

Acknowledgements

I would like to thank my supervisors, professors Ana Marques and Anton Friedl, for all the guidance and help that they gave me through the realization of this work. Furthermore, I would like to address a special thanks to my supervisors for giving me the opportunity to perform this work abroad, allowing me to experience a new culture in a new university in a foreign country, TU Wien in Austria.

This work was carried out at the Institute of Chemical, Environmental and Bioscience Engineering, which I would like to thank to everyone that works in the department, specially to Martin Miltner, Angela Miltner, Johannes Adamecyk, Sebastian Serna, Sarah Keck and Sofia Capelo, for giving me a good, helpful and friendly environment to work. Furthermore, I would like to thank the people I've mentioned and friends that I've made through my journey in Vienna, Anja Dakić, Katarina Knežević, Johannes Niel, Martin Brenner, Alexander Pal, Büsra Çiçek, Kouesaan Aziaba, Joana Barros and Andreia Pereira for making this past seven months one of the best experience of my life and, also, for making me feel like I was at home.

Finally, I'm grateful to my family and closest friends that always supported me, specially my mother that is the person that made all my academic journey possible and has been my rock through all these years.

Abstract

Lignocellulosic biomass is the most abundant renewable resource in the world and has a lot of potential to produce chemicals and biomaterials. Lignin makes part of lignocellulosic biomass and is the second most abundant biopolymer in the world. The lignin retrieved from processes (i.e. paper production process) is typically used in incineration processes to produce energy, but it is possible to use lignin to produce high added value materials, which might require its functionalization.

Therefore, the aim of this work is to provide modified lignin obtained from wheat straw, with a specific organic functionality, by using 3-(trimethoxysilyl)propyl methacrylate (MSPM), to make it more suitable to substitute reagents derived from fossil sources in chemical processes. One example of chemical process is the copolymerization of lignin with acrylonitrile to produce carbon fiber precursors.

The first step of this work was the extraction of lignin through the Organosolv Pre-treatment, followed by processes of precipitation and diafiltration to obtain a cleaned suspension of nanoparticles of lignin. Then, the functionalization process was carried out, consisting of the reaction of the nanoparticles with the MSPM, for different parameters (i.e. temperature, time, dilution and amount of reagent). The nanoparticles of lignin were characterized through analytical methods like phosphorous-31 nuclear magnetic resonance ($^{31}\text{P-NMR}$), Fourier-transformed infrared spectroscopy (FTIR) and scanning electron microscopy (SEM) before and after functionalization.

In conclusion, according to the results obtained from the characterization, the functionalization with the MSPM was achieved but not in its fullness, leaving some space for optimization. The optimal conditions for a successful functionalization with smaller and regular modified lignin nanoparticles are higher temperatures, good stirring achieving perfect mixture, excess of water and excess of MSPM in order to guarantee the reaction of all the OH groups in the lignin.

Keywords: lignin, nanoparticles, functionalization, Organosolv, wheat straw

Resumo

Biomassa lignocelulósica é a fonte renovável mais abundante no mundo e tem imenso potencial para produzir químicos e biomateriais. A lignina faz parte da biomassa lignocelulósica e é o segundo bio polímero mais abundante do mundo. O uso comum de lignina recolhida de processos é a produção de energia a partir de processos de incineração, no entanto, é possível utilizar a lignina para produzir produtos de alto valor, que pode requerer a funcionalização da mesma.

Portanto, o objetivo deste trabalho é providenciar lignina modificada, obtida a partir de palha de trigo, usando γ - Metacrilóxi propil trimetóxi silano (MSPM), de forma a que esta possa substituir reagentes derivados de combustíveis fósseis em processos químicos. Um exemplo de um processo químico é a copolimerização da lignina com acrilonitrila para a produção de precursores de fibras de carbono.

O primeiro passo deste trabalho foi a extração da lignina da palha de trigo usando o pré-tratamento Organosolv, seguido de processos de precipitação e filtração para produzir uma suspensão limpa de nanopartículas de lignina. Depois, foi feita a funcionalização que consistiu em reagir as nanopartículas com o reagente em questão, com diferentes parâmetros (ex. temperatura, tempo, diluição e quantidade do reagente). As nanopartículas de lignina foram caracterizadas por espectroscopia de infravermelho por transformada de Fourier em reflexão atenuada (FTIR-ATR), microscopia eletrônica de varrimento (MEV) e espectroscopia de ressonância magnética nuclear (RMN) antes e depois da funcionalização.

Em conclusão, de acordo com os resultados obtidos da caracterização realizada, a funcionalização com o MSPM foi alcançada, mas não na sua totalidade, havendo espaço para a sua otimização. As condições ótimas para ter uma funcionalização bem-sucedida e com nanopartículas de lignina mais pequenas e regulares, quanto à forma, são temperaturas elevadas, boa agitação atingindo uma mistura perfeita, excesso de água e excesso de reagente para garantir a reação de todos os grupos OH presentes na lignina.

Palavras Chave: lenhina, nanopartículas, funcionalização, Organosolv, palha de trigo

Index

| | |
|---|-----|
| Acknowledgements | iii |
| Abstract | v |
| Resumo | vii |
| List of Figures | 3 |
| List of Tables | 5 |
| List of Acronyms and Nomenclature | 6 |
| Acronyms | 6 |
| Nomenclature..... | 7 |
| 1. Introduction | 8 |
| 1.1. Goal of the Thesis | 9 |
| 1.2. Structure of the Thesis | 9 |
| 2. Literature Review | 11 |
| 2.1. Biorefinery | 11 |
| 2.2. Lignocellulosic Biomass | 12 |
| 2.2.1. Cellulose..... | 13 |
| 2.2.2. Hemicellulose..... | 14 |
| 2.2.3. Lignin..... | 14 |
| 2.2.3.1. Structure and Chemical Composition of Lignin..... | 15 |
| 2.2.3.2. Properties..... | 16 |
| 2.2.4. Pre-treatments of Lignocellulosic Biomass | 17 |
| 2.2.4.1. The Kraft Process | 17 |
| 2.2.4.2. The Sulfite Process..... | 17 |
| 2.2.4.3. The Soda Process | 18 |
| 2.2.4.4. The Organosolv Process..... | 18 |
| 2.3. Production of Lignin Nanoparticles (LNPs)..... | 18 |
| 2.3.1. Applications of Lignin Nanoparticles (LNPs)..... | 20 |
| 2.3.2. Functionalization of Lignin Nanoparticles (LNPs) | 22 |
| 2.3.3. Evolution of the Bonds..... | 24 |
| 3. Materials and Methods | 25 |
| 3.1. Materials..... | 25 |

| | | |
|----------|--|----|
| 3.2. | Experimental Methods | 25 |
| 3.2.1. | Production of Lignin Nanoparticles (LNPs)..... | 25 |
| 3.2.1.1. | Extraction Process, Orgonosolv pre-treatment..... | 26 |
| 3.2.2.3. | Precipitation of Lignin Nanoparticles (LNPs)..... | 29 |
| 3.2.2.4. | Diafiltration of the Precipitate..... | 30 |
| 3.2.2. | Functionalization of Lignin Nanoparticles (LNPs) | 32 |
| 3.2.2.1. | Hydrolysis of the Reagent | 32 |
| 3.2.2.2. | Preliminary Reactions | 34 |
| 3.2.2.3. | Functionalization..... | 34 |
| 4. | Characterization Methods..... | 37 |
| 4.1. | ³¹ P-NMR-spectroscopy | 37 |
| 4.2. | FTIR-spectroscopy..... | 39 |
| 4.3. | SEM | 40 |
| 5. | Results and Discussion..... | 41 |
| 5.1. | Results from Reactions | 41 |
| 5.1.1. | Preliminary Reactions | 41 |
| 5.1.2. | Functionalization..... | 42 |
| 5.2. | Results from Characterization Methods | 45 |
| 5.2.1. | ³¹ P-NMR | 45 |
| 5.2.2. | FTIR-spectroscopy..... | 48 |
| 5.2.2.1. | Measurement Performed on the Lignin Nanoparticles (LNPs) | 48 |
| 5.2.2.2. | Measurements Performed on MSPM and Hydrolysed MSPM..... | 50 |
| 5.2.2.3. | Measurements Performed on the Products of the Functionalization | 53 |
| 5.2.3. | SEM | 58 |
| 5.2.3.1. | SEM performed on the Lignin Nanoparticles (LNPs)..... | 58 |
| 5.2.3.2. | SEM performed on the Products of the Functionalization | 59 |
| 6. | Conclusion..... | 62 |
| | References..... | 64 |
| | Annex A – Block Diagram from the Overall Process | 67 |
| | Annex B – Spectrums from FTIR measurements with the respective peaks for each sample | 68 |

List of Figures

| | |
|---|----|
| Figure 1. Feedstocks and their roots in order to achieve valuable products. The dashed routs are the less efficient connections taken from [1]..... | 11 |
| Figure 2. Adaptation of the table presented in [10] about the general classification of biomass. | 13 |
| Figure 3. Lignin distribution in lignocellulosic biomass taken from [13]. | 15 |
| Figure 4. Structure of the monolignol monomers species present in lignin taken from [13]. | 15 |
| Figure 5. Example of the lignin structure with the main linkages: β -O-4', β -5, β - β' , α -O-4', 4-O -5', 5-5 and β -1' bonds taken from [12]. | 16 |
| Figure 6. Schematic of the different methods able to turn raw lignin into nano- and microparticles. The size range represented is for the successfully synthesized structures taken from [3]. | 19 |
| Figure 7. Schematic of the process of production of nanoparticles used, solvent shifting taken from [12]. | 20 |
| Figure 8. Overview of the several potential applications of lignin nano- and microparticle taken from [2]. | 21 |
| Figure 9. Overview of the reactions used for the functionalization of hydroxyl groups adapted from [12]. | 23 |
| Figure 10. Sample of the wheat straw used in the process. | 25 |
| Figure 11. Representation of the autoclave used in the extraction process. | 27 |
| Figure 12. Representation of the press and centrifuge used in the extraction process. | 27 |
| Figure 13. Operation conditions for one extraction of wheat straw. | 28 |
| Figure 14. Vessel used for storage of extractions. | 28 |
| Figure 15. Left: vessel containing wheat straw before extraction; Right: vessel containing wheat straw dried after extraction. | 29 |
| Figure 16. Precipitation setup. | 30 |
| Figure 17. Setup of the operation of the diafiltration. | 31 |
| Figure 18. Demonstration of an unsuccessful (left) and successful (right) hydrolysis of the reagent. | 33 |
| Figure 19. Setup used for the scale up of the functionalization reactions. | 36 |
| Figure 20. Picture of the lyophilizer used to prepare the samples. | 39 |
| Figure 21. Equipment used for the FTIR measurements. | 39 |
| Figure 22. Equipment used for the SEM analysis. | 40 |
| Figure 23. Product from reactions IIa, IIIa, IIb, IIIb at 25°C and solution I. | 41 |
| Figure 24. Product from reactions IIa, IIIa, IIb, IIIb at 50°C and solution I. | 41 |
| Figure 25. Product from reaction Va, VIa, VIIa and VIIIa at 25°C and solution IV. | 43 |
| Figure 26. Product from reaction Va, VIa, VIIa and VIIIa at 50°C and solution IV. | 43 |
| Figure 27. Product from reaction Vb, VIb, VIIb and VIIIb at 25°C and solution IV. | 44 |
| Figure 28. Product from reactions Vb, VIb, VIIb and VIIIb at 50°C and solution IV. | 44 |
| Figure 29. P-NMR results performed at CS. | 46 |
| Figure 30. P-NMR results performed at washed CS. | 47 |
| Figure 31. Spectra obtained from the FTIR performed on the LNPs from the CS. | 49 |
| Figure 32. Spectra obtained from the FTIR performed on the MSPM. | 51 |
| Figure 33. Spectra from the FTIR performed on the reagent and the hydrolysed reagent. | 52 |
| Figure 34. Comparison between the spectra obtained of reactions Va, VIa, VIIa and VIIIa at 25°C and spectra obtained of LNPs and hydrolysed MSPM. | 54 |

| | |
|--|----|
| Figure 35. Comparison between the spectra obtained of reactions Va, VIa, VIIa and VIIIa at 50°C and spectra obtained of LNPs and hydrolysed MSPM..... | 54 |
| Figure 36. Comparison between the spectra obtained of reactions Vb, VIb, VIIb and VIIIb at 25°C and spectra obtained of LNPs and hydrolysed MSPM..... | 56 |
| Figure 37. Comparison between the spectra obtained of reactions Vb, VIb, VIIb and VIIIb at 50°C and spectra obtained of LNPs and hydrolysed MSPM..... | 56 |
| Figure 38. Photomicrographs of LNPs in the CS at 100 000 magnitude. | 58 |
| Figure 39. Photomicrographs of the MLNPs for the reactions IIa (top left), IIIa (down left), VIIa (top right) and VIIIa (down right), all at 25°C, for 1 h..... | 59 |
| Figure 40. Photomicrographs of the MLNPs for the reactions Va (top left), VIa (down left), VIIa (top right) and VIIIa (down right), all at 25°C, for 1 h..... | 60 |
| Figure 41. Block diagram from the overall process study in this thesis. | 67 |
| Figure 42. Spectra from FTIR measurement on the LNPs. | 68 |
| Figure 43. Spectra from FTIR measurement on the MSPM..... | 69 |
| Figure 44. Spectra from FTIR measurement on reaction Va at 25°C..... | 69 |
| Figure 45. Spectra from FTIR measurement on reaction Va at 50°C..... | 70 |
| Figure 46. Spectra from FTIR measurement on reaction Vb at 25°C..... | 70 |
| Figure 47. Spectra from FTIR measurement on reaction Vb at 50°C..... | 71 |
| Figure 48. Spectra from FTIR measurement on reaction VIa at 25°C..... | 71 |
| Figure 49. Spectra from FTIR measurement on reaction VIa at 50°C..... | 72 |
| Figure 50. Spectra from FTIR measurement on reaction VIb at 25°C. | 72 |
| Figure 51. Spectra from FTIR measurement on reaction VIb at 50°C. | 73 |
| Figure 52. Spectra from FTIR measurement on reaction VIIa at 25°C. | 73 |
| Figure 53. Spectra from FTIR measurement on reaction VIIa at 50°C. | 74 |
| Figure 54. Spectra from FTIR measurement on reaction VIIb at 25°C. | 74 |
| Figure 55. Spectra from FTIR measurement on reaction VIIb at 50°C. | 75 |
| Figure 56. Spectra from FTIR measurement on reaction VIIIa at 25°C..... | 75 |
| Figure 57. Spectra from FTIR measurement on reaction VIIIa at 50°C..... | 76 |
| Figure 58. Spectra from FTIR measurement on reaction VIIIb at 25°C..... | 76 |
| Figure 59. Spectra from FTIR measurement on reaction VIIIb at 50°C..... | 77 |

List of Tables

| | |
|--|----|
| Table 1. Experiments conducted to test the hydrolysis. | 33 |
| Table 2. Identification of the solutions used for the preliminary reactions. | 34 |
| Table 3. Identification of the preliminary reactions and experimental conditions. | 34 |
| Table 4. Identification of the solutions used for the functionalization reactions. | 35 |
| Table 5. Identification of the solutions used for the functionalization reactions. | 35 |
| Table 6. Integration of the functional groups, adapted from [24, 25]. | 38 |
| Table 7. Values found in literature for the quantification of OH groups in lignin through ³¹ P-NMR. | 48 |
| Table 8. Assignments of FTIR measurement on LNPs, adapted from previous studies [20, 29–33]. | 50 |
| Table 9. Assignments of FTIR measurement on MSPM, adapted from previous studies [20, 30, 34–37]. | 52 |
| Table 10. Ratio Si-OH/Si-O-C calculated with the data retrieved from FTIR analysis on each reaction. | 57 |

List of Acronyms and Nomenclature

Acronyms

AA – Acetic acid

ATR – Attenuated total reflectance

CDCl₃ – Deuterated chloroform

CS – Clean suspension of LNPs

DMF – Dimethylformamide

EHL – Steam explosion lignin and enzymatic hydrolysis lignin

FTIR – Fourier-transform infrared spectroscopy

GHG – Greenhouse gas

IPCC – Intergovernmental Panel on climate change

KL – Kraft lignin

LNPs – Lignin nanoparticles

LS – Soda lignin, lignosulphonates

MDI – 4,4'-diphenyl methane diisocyanate

MLNPs – Modified lignin nanoparticles

MSPM – 3-(trimethylsilyl) propyl methacrylate

OS – Organosolv lignins

pDNA – plasmid DNA

³¹P-NMR – Phosphorous-31 nuclear magnetic resonance

SEM – Scanning electron microscopy

TBDMS – *tert*-butyldimethylsilyl

TBDMSCl – *tert*-butyldimethylsilyl chloride

THF – tetrahydrofuran

TMDP – 2-chloro-4,4,5,5-tetramethyl-1,3,2-dioxaphospholane

UV – Ultraviolet

Nomenclature

Ca – Calcium

CH₂ – Methylene

CH₃ – Methyl

CH₄ – Methane

CO₂ – Carbon dioxide

C_{standard} – Concentration of cyclohexanol standard used in the ³¹P-NMR [mg/mL]

G – Guaiacyl units

h – hours

H – p-hydroxyphenyl units

I (900-800 cm⁻¹) – peak intensity or area of Si-O-C bond

I (1030-1010 cm⁻¹) – peak intensity or area of Si-OH bond

I_{func.gr.} – Integral of corresponding lignin functional group in defined integration area

I_{standard} – Integral of cyclohexanol standard for the ³¹P-NMR

K – Potassium

Mg – Magnesium

min – minutes

m_{sample} – Mass of the lignin sample used in ³¹P-NMR [mg]

M_{standard} – Molecular mass of cyclohexanol standard [g/mol]

M_w – Molecular weight [Da]; [g/mol]

nm – nanometres

Si – Silicon

T_g – Glass transition temperature [°C]

wt % – Weight percentage of mixture

µm – micrometres

1. Introduction

Fossil sources, more precisely, crude oil dominated the second half of the 20th century as the raw material for energy, transportation and chemicals. Even though the source of fossil fuels is limited, the processing technologies have been developed since the 1860s with high demand until the so-called “peak oil”. As it is well known, the threat of global warming is increasing and consequentially the public awareness that reflects on the exploration of alternatives to fossil fuels. [1]

Lignocellulosic biomass is the most abundant renewable source in the world and has a lot of potential to produce chemicals and biomaterials. After cellulose, lignin is the second most abundant biopolymer on earth and 40% of it is used for the demand of internal energy of a biorefinery meaning that the rest can be used for other purposes that add value to biomass increasing its economic value. Lignin is a highly irregularly branched polyphenolic polyether, consisting of the primary monolignols, p-coumaryl alcohol, coniferyl alcohol and sinapyl alcohol, which are connected via aromatic and aliphatic ether bond as well as non-aromatic C-C bonds. There are three different types of lignins: softwood lignins that are composed of coniferyl alcohol, hardwood lignins that have coniferyl and sinapyl alcohol and grass lignins of all three types. This unique structure makes lignin appealing to the production of new products, but there are some challenges to be overcome in the process and valorisation of it regarding its intricacy and inhomogeneity. [2]

One way to move past the complexity of the lignin is to resort to the production of lignin nanoparticles (LNPs), because nanostructured materials, especially in the 1-100 nm range, can offer unique properties due to their increased surface area and considerably different properties than a larger-dimensional material of the same composition. In the past years, the preparation of LNPs has gained a lot of interest for applications like the improvement of mechanical properties, bactericidal and antioxidant properties and impregnations to drug carriers for hydrophobic and hydrophilic substances. [3]

Before the production of nanoparticles, it is necessary to fractionate the lignocellulosic raw materials, which can be done by several pre-treatments. The Organosolv pre-treatment has the advantages of obtaining separation of high purity cellulose with minor degradation, isolation of high-quality lignin and higher efficiency of hemicellulose fractionation compared to other conventional treatments. This method uses organic or aqueous-organic solvents with or without addition of a catalyst (acid, base or salt) to hydrolyse the lignin bonds and lignin-carbohydrate bonds, resulting in a solid residue composed mainly by cellulose and some hemicellulose. The most popular solvent used for this process is ethanol, however, methanol, acetone, formic acid, acetic acid and glycerol are also good options to be considered. [4]

The production of nanoparticles can be done in different ways that can be distinguished by the production method and subsequently by the shape of the product. Solvent shifting is one efficient method to use in the liquid product of the Organosolv method and includes the addition of an excess of water to it that generates nanoparticles with the decrease of solubility. From this process it is possible to obtain solid or hollow spherical-like particles. [2]

In order to obtain a cleaned suspension (CS) of lignin from the product of the precipitation, it is required to use a process of separation that can remove the impurities. The ultrafiltration is a process that feeds a module with a membrane inside with the help of a pump. The fluid passing the membrane is diverted as permeate and the fluid retained by the membrane is diverted as retentate, the CS of lignin. [5] It is possible to optimize the time of the ultrafiltration by turning it into a diafiltration process by adding water to the feed tank, decreasing the concentration of solids and therefore, helping the passage of the fluid through the membrane preventing clogging.

As said previously, LNPs have gain interest over the years but since lignin is a highly complex biopolymer, there has been some work performed in the field of the functionalization of these particles. The functionalization of lignin consists in reacting the OH groups present in it with other chemicals towards improving the quality of lignin and trying to make it suitable for several applications, for example, carbon fibers precursors.

In this dissertation, the following studies were carried out for the production of a CS of LNPs in water: the Organosolv pre-treatment with a 60 w/w % aqueous ethanol solution at 180°C, a direct precipitation using water as an antisolvent and, finally, a diafiltration process to obtain a CS of LNPs in water. This was followed by the functionalization of the nanoparticles with the help of a methacrylate silane: 3-(trimethoxysilyl)propyl methacrylate (MSPM).

1.1. Goal of the Thesis

Lignin is a byproduct from the pulp and paper industry or from cellulosic biorefineries. Its aromatic building blocks make it an attractive feedstock of direct synthesis of specialty aromatic chemicals. This work deals with lignin nanoparticles (LNPs) which, due to their higher surface area than standard lignin, exhibit enhanced properties, originating higher added value applications.

The main goal of the thesis is to obtain LNPs and provide them an organic functionalization, via sol-gel processing, using a methacrylate silane (vinyl groups), which enable the copolymerization of the modified LNPs with other monomers.

This effort will be starting point for their utilization in the production of a new generation of acrylic fibers or as precursors for high value carbon fibers.

1.2. Structure of the Thesis

This thesis is composed by seven chapters. Chapter 1 presents the framing of the thesis, a brief introduction, the goal of the thesis and the explanation of the work performed in it.

Chapter 2 presents the literature review of the topics referred in the written paper.

Chapter 3 describes the materials and the experimental methods implemented in this thesis.

Chapter 4 mentions every characterization process used and is accompanied with a description of each of them.

Chapter 5 refers to the results and discussion of every step of the work done for this thesis.

At last, in chapter 6 shows the conclusions that were possible to retrieve from the work performed.

2. Literature Review

2.1. Biorefinery

Surviving in the planet Earth with limited resources to support the increasing global population is the greatest challenge for humanity. This challenge is aggravated by the fact that the global economy is driven by technologies that are not sustainable, using petrochemical feedstock. [6]

The humanity strong dependence on fossil fuels combined with the diminishing petroleum resources are causing environmental and political concerns. According to the Intergovernmental Panel on Climate Change (IPCC) Fourth Assessment Report, the world's growing population and per capita energy demand are leading to the increase in greenhouse gas (GHG) emissions. The GHG emissions, more particularly, carbon dioxide (CO₂), methane (CH₄) and nitrous oxide (N₂O) are caused mainly by the combustion of fossil fuels and this combined with other human activities are disturbing the Earth's Climate. [7]

The world's primary source of energy for the transport sector and production of chemicals sector is oil, whose consumption is expected to be about 116 million barrels a day by 2030. In order to reduce the dependence on oil and, consequently, intervene in the climate change in a good way, alternative chains of production are being approached. Processes based in renewable raw materials (i.e. biomass) have the potential to replace plants bases on fossil fuels in the production of energy and non-energy (i.e. chemicals and materials) sectors. [7]

The public opinion and the increasing threat of global warming made governments act into looking for alternatives to fossil fuels. The key point is to substitute the feed in order to produce the same: energy, transportation fuels and chemicals. Biorefineries using biomass can be able to process different biomass feedstocks to obtain the same and/or equivalent products as those obtained from oil. [1]

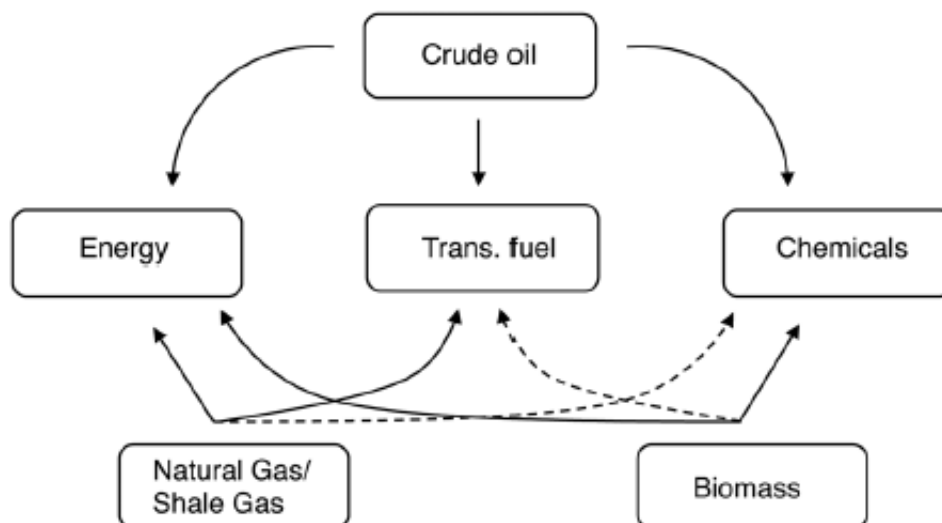


Figure 1. Feedstocks and their roots in order to achieve valuable products. The dashed routes are the less efficient connections taken from [1].

Compared to fossil fuels, biomass is over-functionalized, has a high oxygen content, is available worldwide and, more important, is renewable on a human timescale. An important point that should be taken into consideration, when developing biorefineries, is that the biomass used in it shouldn't compete with the food sectors harming its economy. [1]

According to the IEA Bioenergy task 42, "biorefining is the sustainable processing of biomass into a spectrum of marketable products and energy". It is a facility that converts biomass into biofuels, power and chemicals being analogous to today's petroleum refinery. These facilities still have some challenges that need to be overcome, like their efficiency and the cost of production. [7]

The first main processes in the biorefinery involved ethanol fermentation for fuels, lactic acid fermentation, propanediol fermentation and the lysine fermentation especially for polymer production. Biorefinery systems based on cereals, lignocelluloses, grass, alfalfa and their optimization are being studied towards improving them. Looking into society nowadays, biorefineries are interesting on the ecological and economical point of view. [8]

Biorefinery industries are in the stage of development world-wide with capacity of revitalize rural areas, providing employment and, more important, they are best bet into fighting the climate change provoked by the release of GHG by using fossil fuels.

2.2. Lignocellulosic Biomass

Biomass can be defined as a material of biological origin excluding material embedded in geologic formation and/or transformed to fossil and it is the largest source of renewable organic material on Earth. Lignocellulosic biomass refers to nonedible plant materials or nonedible parts of plants made up primarily of cellulose, hemicelluloses and lignin. It includes agricultural residues, forestry residues, a fraction of municipal and industrial wastes and energy crops. These resources typically contain on dry weight basis 40-60% cellulose, 20-40% hemicelluloses and 10-25% lignin and these three components are the main structural component of plant cell walls. [9, 10]

Beside the three main components, biomass has a small fraction of organic solvents (i.e. ethanol, acetone, dichloromethane and benzene). These components are called extractives and belong to a heterogeneous group including waxes, fatty acids, gums, resins, chlorophyll, terpenoids and a variety of phenolic substances, among others. They act as metabolic intermediates, energy storage or act as mechanism of defence against microbial attacks. Regarding the physical characteristics of the biomass, they are responsible for colour, smell and resistance to wilt. [10]

Another component present in biomass, is ash, which is composed by several inorganic compounds (i.e. calcium (Ca), potassium (K), magnesium (Mg) and silicon (Si)). The next figure was retrieved from [10] and represents the general classification of biomass with its respective composition.

| General Biomass Classification | Lignocellulosic Biomass Type | Cellulose | Hemicellulose | Lignin |
|--------------------------------------|----------------------------------|--------------|---------------|-----------|
| Hardwood | American sycamore | 37.2–41.8 | 17.6–19.6 | 25.0–27.3 |
| | Black locust | 39.3–42.6 | 16.6–18.9 | 24.4–28.6 |
| | Eucalyptus | 46.6–50.3 | 12.7–14.4 | 26.9–28.2 |
| | Hybrid poplar | 40.3–47.3 | 16.6–22.6 | 15.5–16.3 |
| | Willow | 42.4–45.3 | 20.6–22.9 | 16.9–18.9 |
| | Oak | 40.4 | 35.9 | 24.1 |
| Softwood | Pine | 42.0–50.0 | 24.0–27.0 | 20.0 |
| | Spruce | 45.5 | 22.9 | 27.9 |
| Agricultural/agroindustrial residues | Sugarcane bagasse | 31.9–43.4 | 12.2–25.5 | 23.1–27.6 |
| | Brewer's spent grains | 16.8–26.0 | 19.2–29.6 | 16.9–27.8 |
| | Spent coffee grounds | 11.6–13.2 | 37.2–41.0 | 22.2–25.6 |
| | Rice straw | 29.2–34.7 | 23.0–25.9 | 17.0–19.0 |
| | Rice husks | 28.7–35.6 | 12.0–29.3 | 15.4–20.0 |
| | Com stover | 30.6–38.1 | 19.1–25.3 | 16.7–21.3 |
| | Com cobs | 33.7–41.2 | 31.9–36.0 | 6.1–15.9 |
| | Com stalks | 35.0–39.6 | 16.8–35.0 | 7.0–18.4 |
| | Wheat straw | 35.0–39.0 | 23.0–30.0 | 12.0–16.0 |
| | Barley hull | 34.0 | 36.0 | 13.8–19.0 |
| | Barley straw | 36.0–43.0 | 24.0–33.0 | 6.3–9.8 |
| | Oat straw | 31.0–35.0 | 20.0–26.0 | 10.0–15.0 |
| | Ray straw | 36.0–47.0 | 19.0–24.5 | 9.9–24.0 |
| | Sorghum straw | 32.0–35.0 | 24.0–27.0 | 15.0–21.0 |
| | Herbaceous crops | Big bluestem | 29.0–37.2 | 20.5–25.8 |
| Sericea lespedeza | | 32.7–39.4 | 15.7–19.4 | 24.1–31.9 |
| Tall fescue | | 23.4–26.4 | 18.2–20.4 | 10.9–14.8 |
| Switchgrass | | 26.8–37.5 | 22.4–28.8 | 13.2–22.5 |
| Miscanthus | | 35.0–40.0 | 16.0–20.0 | 20.0–25.0 |
| Other waste | Tobacco chops | 22.0–30.0 | 15.0–20.0 | 15.0–25.0 |
| | Cellulose sludge | 31.4 | 9.8 | 15.3 |
| | Agave whole residue | 30.7 | 16.9 | 16.9 |
| | Waste papers from chemical pulps | 60.0–70.0 | 10.0–20.0 | 5.0–10.0 |
| | Solid cattle manure | 1.6–4.7 | 1.4–3.3 | 2.7–5.7 |

Figure 2. Adaptation of the table presented in [10] about the general classification of biomass.

Lignocellulosic biomass is appealing for biorefineries because it is highly available, has a low price and possesses a high content of polysaccharides.

2.2.1. Cellulose

Cellulose is the most abundant biopolymer on earth, is a homopolysaccharide composed of parallel unbranched β -1,4-linked *glucan* chains that form microfibrils. The small repetitive unit of cellulose is cellobiose and has the possibility to be converted into glucose residues.

The microfibrils of $\cong 3$ nm in higher plants consist on well-packed, long hydrogen-bonded stretches of crystalline cellulose and less ordered amorphous regions. These are the main component of the cell wall in plants. [9, 11]

2.2.2. Hemicellulose

Hemicelluloses are a heterogeneous group of matrix polymers of low molecular weight, they are branched polysaccharides that have mostly β -1,4-linked backbones with an *equatorial configuration*. The matrix is built up by pentoses (*D*-xylose, *D*-arabinose), hexoses (*D*-mannose, *D*-glucose, *D*-galactose) and sugar acids.

Regarding cell walls, hemicelluloses constitute matrix polysaccharides together with pectins in primary cell walls, while for secondary cell walls they are the matrix polymers with lignin. Also, they are bind to the surface of the cellulose microfibrils and to each other by hydrogen bonding. Their most important characteristic is that they contribute for the strengthening of the cell wall by interacting with cellulose and lignin. [9, 11]

2.2.3. Lignin

Like mentioned before, lignocellulosic biomass contains approximately on dry weight basis 40-60% cellulose, 20-40% hemicelluloses and 10-25% lignin and they are the main components of plant cell walls. Lignin acts primarily as a structural component since it gives strength to the wall, provides physical barrier against attacks by phytopathogens and prevents the degradation of structural polysaccharides. [9, 12]

Lignin is the second most abundant biopolymer on earth and represents 30% of the organic carbon in biosphere. There are three types of lignin: softwood lignins that are mainly coniferyl alcohol, hardwood lignins composed by coniferyl and sinapyl alcohol and grass lignins that conjugates all three types (p-coumaryl, coniferyl and sinapyl alcohol). [3]

From the lignin generated nowadays, 40% is used to cover the internal energy demand of a biorefinery, while the remaining 60% are available to be used in valorisation processes to produce high value products. This valorisation of lignin can affect biobased economy in a positive way by improving the utilization of biomass in process and consequently increasing the economic value. [2]

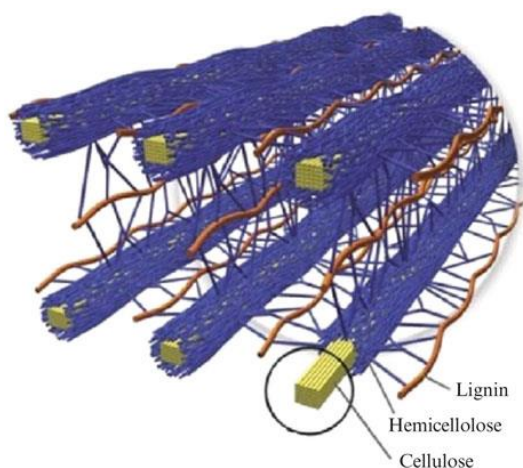


Figure 3. Lignin distribution in lignocellulosic biomass taken from [13].

2.2.3.1. Structure and Chemical Composition of Lignin

Lignin is a physically and chemically heterogeneous macromolecule that is made from phenylpropanoid units that are the oxidative polymerization of three types of hydroxycinnamoyl alcohol sub-units, known as monolignols: *p*-coumaryl, coniferyl and sinapyl alcohols. When these compounds are incorporated in the lignin polymer, each monolignol originates *p*-hydroxyphenyl (H), guaiacyl (G) and syringyl (S) units with structural differences in the extent of methoxylation at the 3' or 3'-5' position of phenolic rings.. [6, 12, 13]

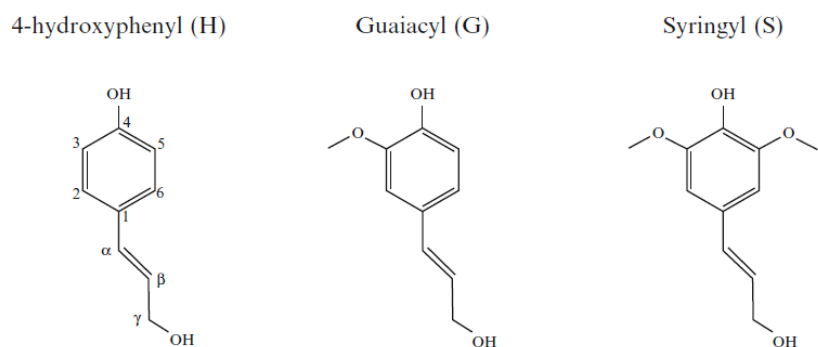


Figure 4. Structure of the monolignol monomers species present in lignin taken from [13].

A series of reactions (hydroxylation, methylation and reduction) conducted by specific enzymes leads to the lignin biosynthesis that is the formation of the polymer with a disorderly and irregular macromolecular structure like the one in Figure 5. The main bonds in lignin are β -O-4' ether linkages that represent more than 50% of its structure. [6, 12, 13]

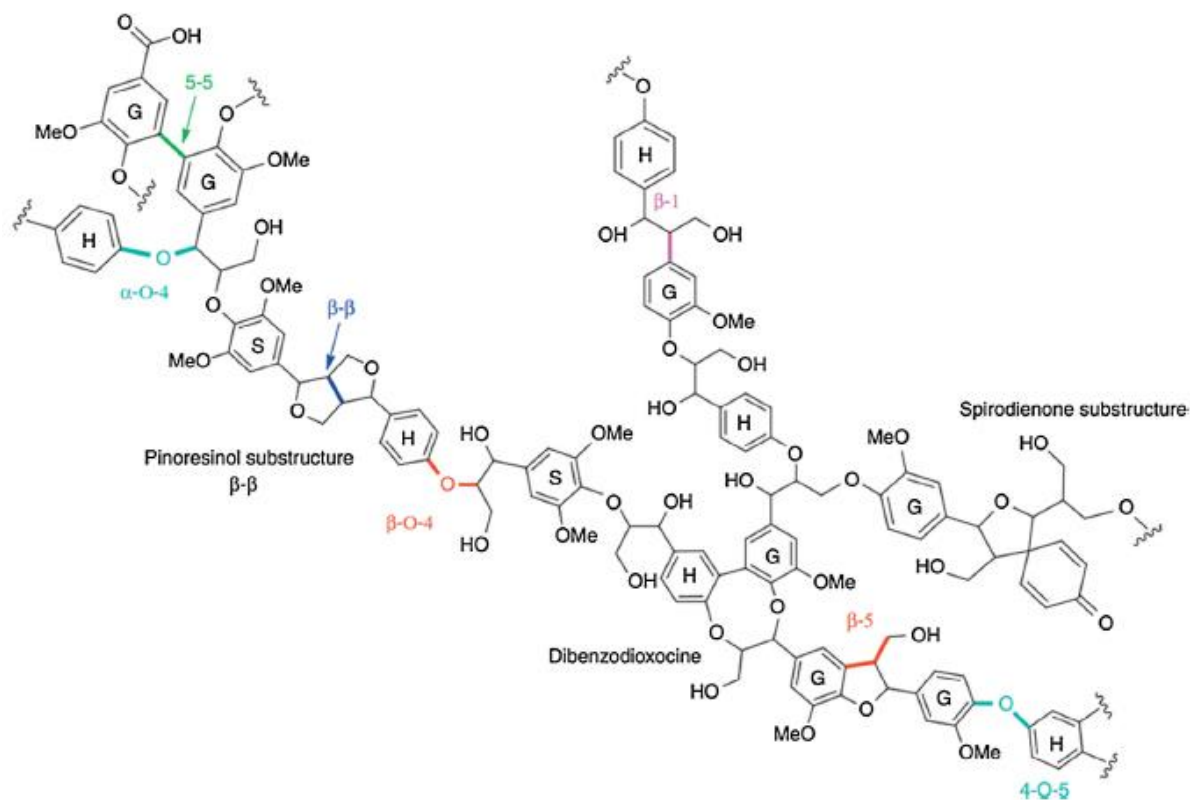


Figure 5. Example of the lignin structure with the main linkages: β -O-4', β -5, β - β ', α -O-4', 4-O-5', 5-5 and β -1' bonds taken from [12].

The composition of lignin is highly dependent on the feedstock and on the extraction process used, meaning that lignins derived from hardwoods have a different composition than lignins derived from softwoods or grass. [10]

Lignin possesses three functional groups: aliphatic OH, phenolic OH and carboxylic OH.

2.2.3.2. Properties

Lignin has several properties and advantages that makes it appealing for industrial purposes, since it has several properties and advantages that other bio renewable polymers possess. Some of the main characteristics and advantages are listed below [12]:

- Antioxidant, antifungal and antimicrobial activities;
- Available in large amounts in industrial waste of by-products;
- Biodegradable and CO₂ neutral;
- Resistant to chemical and biological attacks;
- Able to absorb UV-radiation and fire-retardant;

- Good rheological characteristics, good viscoelastic properties, film-forming capacity and compatibility with a wide range of chemicals.

Furthermore, since lignin is an amorphous polymer, the glass transition temperature (T_g) is one of the best properties to describe it, ranging between 110 and 150°C. As it was mentioned before, there are some challenges to be overcome regarding lignin, being one of those its solubility. Lignin is insoluble in several organic solvents, however, it is possible to change this feature by changing its molecular structure. [6]

2.2.4. Pre-treatments of Lignocellulosic Biomass

There are several processes to extract lignin from lignocellulosic biomass, but the resulted lignin can be classified as: Kraft lignin (KL), Soda lignin, lignosulphonates (LS), Organosolv lignins (OS), Steam-explosion lignin and enzymatic hydrolysis lignin (EHL). [3]

Regarding industry, there are four processes that are the most used ones and the most interesting ones, being described in the following sub-chapters.

2.2.4.1. The Kraft Process

The Kraft process is the most common one being responsible for 85% of produced lignin in the industry. The traditional delignification process is performed by dissolving the lignin in sodium hydroxide and sodium sulfide at a pH range of 13-14, this will increase the phenolic hydroxyl groups that will start to ionize allowing to solubilize the lignin. In order to isolate the lignin from the alkaline solution, it is used an acid (e.g. sulfuric acid), lowering the pH to 4-7.5.

The Kraft lignin resulting from this process it is only soluble at $\text{pH} > 10$, therefore it requires a sulfonation to make it soluble in water. It possesses small amounts of sulfur groups (1 - 3% by weight) and has a molecular weight (M_w) comprehended between 1000 and 3000 Da. [12]

2.2.4.2. The Sulfite Process

This process consists in reacting lignin with a metal sulphite and sulfur dioxide, with calcium, magnesium or sodium acting as counter ions. The operating conditions are a pH between 2 and 12, a temperature between 120°C and 180°C and a digestion time of 1 - 5 h. By applying these conditions, a sulfonic acid group is added to the lignin backbone enabling its hydrolysis and dissolution (cellulose remains solid), producing a lignin with a sulfur content between 4 and 8% by weight and a M_w between 1000 and 50000 Da. There are some disadvantages related with this process, being those the formation of new C-C bonds altering the lignin's structure and the presence of ash and other impurities in it. [12]

2.2.4.3. The Soda Process

The soda process is similar to the Kraft process, since the biomass is digested at a range of temperature between 140 and 170°C with an aqueous solution of sodium hydroxide of 13 to 16% by weight. Also, there is the adding of anthraquinone as a catalyst to decrease the degradation of carbohydrates and, more important, to dissolve the lignin. This process can take several hours and has a high downstream enzymatic efficiency. The lignin obtained from it has a M_w between 1000 and 3000 Da and it is free of sulfur, which is a huge advantage comparing it with the Kraft and Sulfite process. [12, 14]

2.2.4.4. The Organosolv Process

The Organosolv process is the one that is the most promising process and is the treatment of the biomass with organic solvents. The conventional solvents used for this process are ethanol, methanol, acetic and formic acid that can be mixed with water or not at a range of temperatures between 170°C to 190°C. There is also the possibility of improving the process by adding basic or acid catalysts.

This process works by dissolving lignin and part of hemicellulose, leaving cellulose as a solid. The recovery process of the lignin can be done by precipitation steps or evaporation of the organic solvent. The advantages of this process consist in preserving the lignin's native structure, making it valuable for valorisation in several chemical processes, making this pre-treatment process the most efficient one in delignifying the biomass. However, since it uses organic solvents it leads to the corrosion of the equipment and to a lower quality of the produced pulp. [12]

For the present project, this was the process used to pre-treat the biomass. It was conducted in a 1 L stirred autoclave with a 60 wt % aqueous solution of ethanol, taking into consideration the water existent in the biomass. The autoclave was heated at 180°C within 45 min and held at this temperature for 15 min, proceeding with a cooling system afterwards. The liquid and solid product obtain were put through a hydraulic press and a centrifuge in order to separate it, being the liquid fraction (containing solubilized lignin) the desired one. [15]

2.3. Production of Lignin Nanoparticles (LNPs)

Lignin is highly available and has good structural potential to create high-value materials, however, its complex macromolecular structure and lack of homogeneity make it an unexplored component. One way to overcome these issues is transforming the lignin obtained from the pre-treatments into nanoparticles of uniform size and shape. [3]

The development of LNPs can improve the properties of polymer blend and give a higher antioxidant activity to it and, more important, it turns lignin more suitable to be chemical modified by changing its functional group. This means that LNPs are more suitable for being functionalized than the raw lignin, which highly increases its market value. [12]

There are several processes that can be used to turn raw lignin into nanoparticles, and they can be summarize by the following figure:

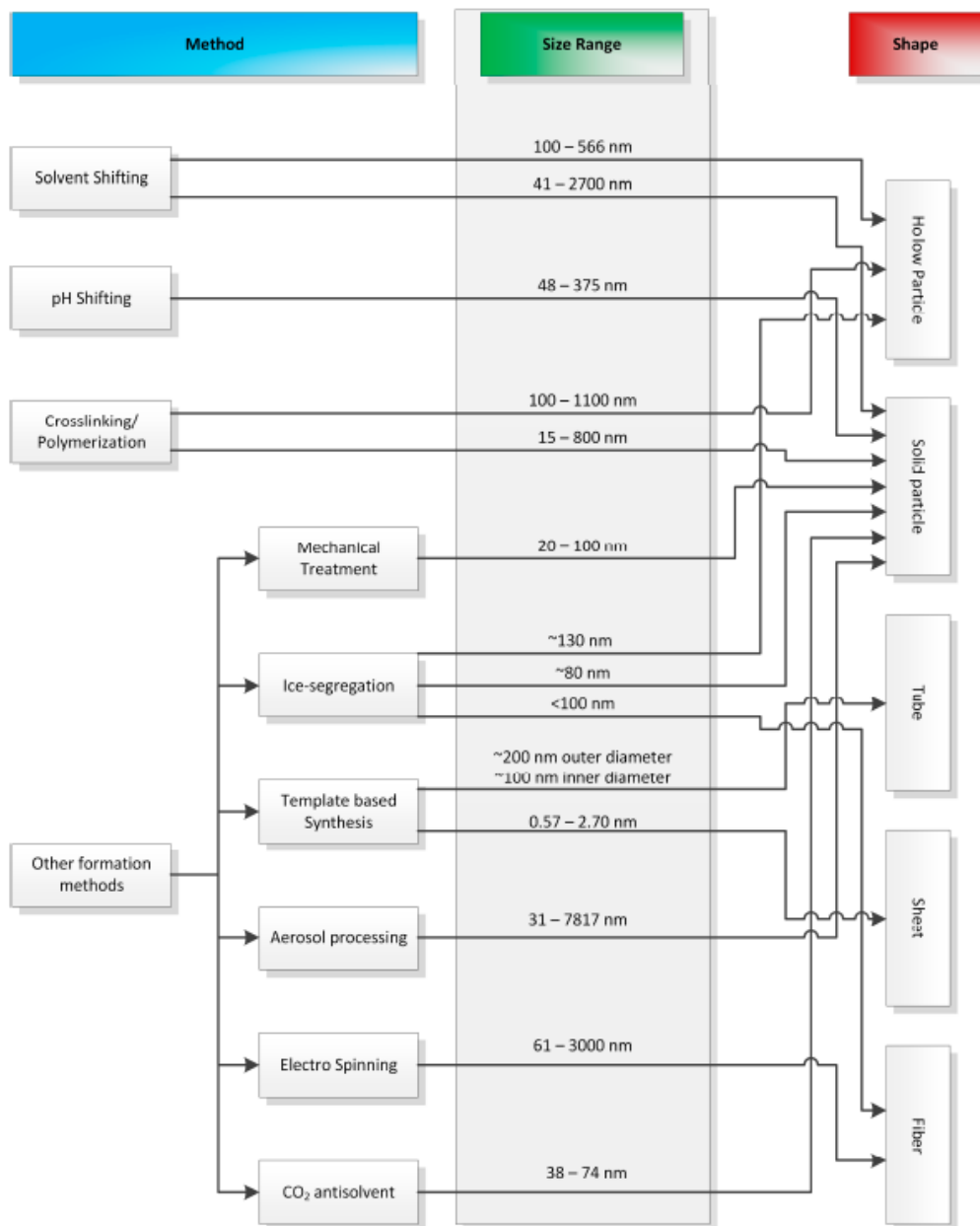


Figure 6. Schematic of the different methods able to turn raw lignin into nano- and microparticles. The size range represented is for the successfully synthesized structures taken from [3].

Applying the Organosolv pre-treatment, the solvent shifting method is the more suitable to the liquid fraction obtained from it and, therefore, was the one used in the present project. This method consists in mixing

the liquid product from the pre-treatment, which is a solution of an organic compound in a water miscible organic solvent, with an excess of water. The water will act as an anti-solvent, decreasing the solubility and making the dissolved lignin precipitate in the form of nanoparticles. This method produces nanoparticles on the range of 41 to 2700 nm. [3]

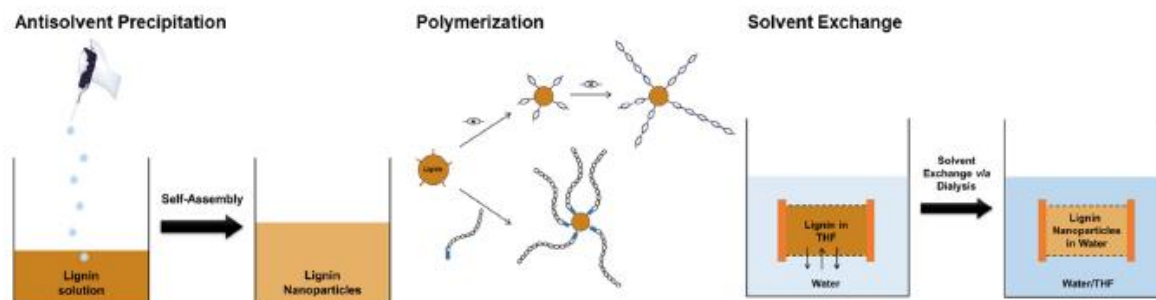


Figure 7. Schematic of the process of production of nanoparticles used, solvent shifting taken from [12].

2.3.1. Applications of Lignin Nanoparticles (LNPs)

The development of LNPs presents key advantages into turning lignin a high-value product with high economic value in the industry. By producing nanoparticles, a new range of applications opens to the valorisation of lignin and these applications can be summarized by the following figure.



Figure 8. Overview of the several potential applications of lignin nano- and microparticle taken from [2].

As it possible to see from Figure 8, the applications of LNPs can be as [2]:

- **Reinforcement:** Using LNPs as nanofillers in several compounds (e.g. foams, membranes) can improve stiffness, strength, toughness, thermal stability and barrier properties;
- **Ultraviolet (UV) Blocker:** Lignin contains UV-absorbing functional groups (i.e. phenolic, ketone and others) and this can be used in sunscreens or textiles, which by applying LNPs improves their effectiveness;
- **Biocide:** Lignin contains different phenolic monomer fragments (their structure consists in the most inhibitory effect) and is a source of natural antibacterial compounds, by using LNPs, the surface is bigger and, therefore, the contact area is bigger and this increases the antimicrobial effect;
- **Antioxidants/Radical Scavengers:** Lignin is an effective free-radical, which can reduce oxygen radicals and retard and inhibit oxidation reactions;

- **Surfactants in Pickering Emulsions:** Pickering emulsions are stabilized by solid particles at the interface between the dispersed phase and the continuous phase, therefore, LNPs are able to stabilize these emulsions;
- **Carbonized Lignin Nano Fibers and Particles:** Lignin can be used as precursor for carbon fibers, opening the possibility of integrating them in supercapacitors, fuel cells, structural composites and filtration devices;
- **Nano- and Microcarrier:** The LNPs can be used in the structure of drug carrier seems in the medical field by carrying the substance encapsulated when they are hollow particles or infused with the carried substance if they are solid and porous particles.

2.3.2. Functionalization of Lignin Nanoparticles (LNPs)

The functionalization of nanoparticles is still a new topic, something that is still being develop and studied, therefore, there are not a vast range of articles supporting this theme.

According to Figueiredo et al., there are four major processes of chemical modification of lignin: lignin depolymerization, synthesis of new chemically active sites, functionalization of hydroxyl groups and production of lignin graft copolymers. Through depolymerization, it is possible to turn lignin raw materials into valorised lignin-based products, including fuels and basic chemicals or oligomers. The other three processes focus on the functional groups of lignin: hydroxyls, methoxyls, carbonyls and carboxyls. [12]

When talking about the synthesis of new chemically active sites, it is referred to the synthesis of new macromonomers that are more effective and reactive by increasing the reactivity of hydroxyl groups or changing the nature of chemically active sites. This can be performed by hydroxyalkylation, amination, nitration, sulfomethylation and sulfonation. [12]

The production of lignin graft copolymers consists in attaching polymer chains to the hydroxyl groups on the lignin structure, leading to the formation of star-like branched copolymer with a lignin core. There are two different methods to elaborate the lignin graft copolymers: “grafting from” and “grafting to” techniques. The first technique uses lignin as macro-initiator for the polymerization, while the monomer reacts with the hydroxyl groups. The second technique implements the synthesis of the polymer chain that needs to be functionalized with an end group and only after, it is able to react with the lignin. [12]

The functionalization of the hydroxyl groups, as the name implies, consists in the modification of the hydroxyl groups, since they are the most reactive functional groups and can affect the chemical reactivity of the newly formed material. Figueiredo et al., refers to some functionalization reactions: alkylation, esterification, etherification, phenolation and urethanization. Each reaction is described in the following figure:

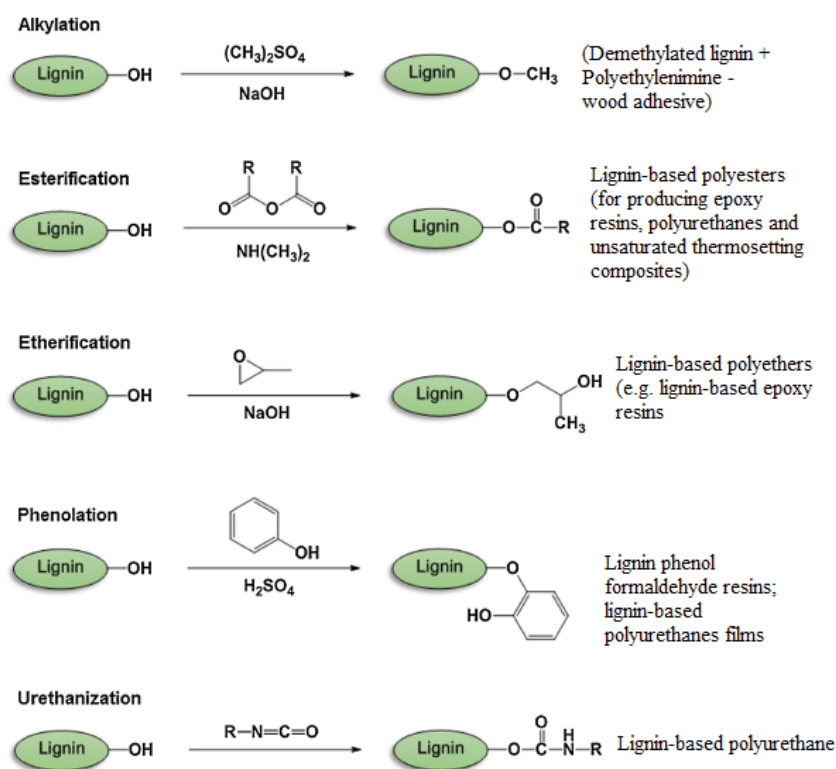


Figure 9. Overview of the reactions used for the functionalization of hydroxyl groups adapted from [12].

Buono et al. performed for the first time the functionalization of soda lignin (SL) with *tert*-butyldimethylsilyl groups (TBDMS) by reaction with *tert*-butyldimethylsilyl chloride (TBDMSCl) using imidazole as catalyst. The silylation was performed by dissolving SL in dimethylformamide (DMF) and then adding the mixture of TBDMSCl and imidazole. The partially silylated products were removed under vacuum followed by a methanol wash and the fully silylated products were recovered after precipitation with water followed by a methanol wash. The modification of SL into Si-SL was successful and confirmed by FTIR, ³¹P-NMR, ¹H-NMR. The Si-SL showed an enhanced thermal stability, hydrophobicity and solubility towards SL and had potential to be used with hydrophobic polymer matrices. Once TBDMSCl is compared with acetic anhydride (that produces similar results, but not as good) it is considered costly, about 10 times more, which is the downside of this whole method. [16]

Chauhan et al. used isocyanate prepolymer for blend preparation with soda lignin (SL) to be used as adhesive in bonding of lingo-cellulosics due to its high cross-linking and plasticity characteristics. The functionalization was performed with 4,4'-diphenyl methane diisocyanate (MDI) with tetrahydrofuran (THF) that was used as the solvent employed to make the reaction occur transforming lignin OH groups into urethanes moieties. Afterwards, the isocyanate prepolymer was created by mixing MDI with 1,4-butanediol and using dibutyl tin dilaurate as catalyst. Finally, the lignin-isocyanate prepolymer blends were achieved with a content of 15 wt % of lignin by mixing vigorously the previous products. The optimal properties of the blends were obtained at 5 – 7

wt % of lignin resulting in a higher glass transition temperature, due to the formation of entanglement of lignin urethanes and cross-links, and more mechanically stable than the parent ones. [17]

He et al. performed LNPs hydrophobization with citric acid as a reagent accompanied by sodium hypophosphite (SHP) being the first. The study was conducted with the goal of producing modified LNPs (MLNPs) using an oversimplified, sustainable, mild and low energy-costing procedure exploring the opportunity of applying functionalized nanofillers as biobased reinforcements in polymer matrix. The LNPs suspension was obtained from alkali lignin by hydrochloric acid treatment, followed by the addition of hydrochloric acid and finally the filtration and dialysis to remove impurities and neutralize the suspension of LNPs. The modification occurred by adding freeze-dried LNPs into 5 wt % of citric acid and 1 wt % for 1 hour and then the solution was filtered, dried and washed with water. In the end, it was obtained a powdered of MLNPs by freeze-drying the suspension. The modification was successful in adding ether groups to it, however, only small parts of the chemical structure were affected by the modification. The MLNPs showed reduced dispersibility in methanol as compared to LNP. Overall, the modification was efficient, and it was proven that the approach used could provide a feasible and convenient method to prepare functionalized nanofillers. [18]

Liu et al. conducted the functionalization of kraft lignin (KL) through esterification of the alcohol and phenol functional groups on lignin backbone with 2-bromo-isobutyric bromide under mild condition: room temperature. This modification was performed successfully to create copolymers capable of compact plasmid DNA (pDNA) into nanoparticles with sizes ranging from 100 to 200 nm. [19]

On this dissertation, the functionalization of the LNPs was performed with a methacrylate silane as a functional group. The main goal was to modify the LNPs by adding a vinyl group to it opening the possibility of using the MLNPs in the production of new generation of acrylic fibers or as precursors for high value carbon fibers.

2.3.3. Evolution of the Bonds

As mentioned before, the functionalization consists in the reaction of the OH groups in the MSPM and the OH groups in the lignin. However, the MSPM does not have OH bonds, so it is necessary to resort to a hydrolysis.

The hydrolysis consists in reacting the Si-OCH₃ bonds with H₂O, forming Si-OH bonds. After the hydrolysis it is possible that the Si-OH bonds react with themselves and form Si-O-Si bonds. The Si-OH bonds that are available, once in contact with lignin, react with the OH groups present in it and form Si-O-C bonds, carrying the vinyl organic functionality, which is the main goal of this thesis.

3. Materials and Methods

3.1. Materials

Lignin was obtained from wheat straw, composed of approximately 93% of dry matter and 7% of water. 3-(trimethoxysilyl)propyl methacrylate (MPMS) of 98% from *Sigma Aldrich*. Ethanol at 99.9% from *Chem-lab*. Acetic acid (AA) at 99.7% from *Sigma Aldrich*.



Figure 10. Sample of the wheat straw used in the process.

3.2. Experimental Methods

3.2.1. Production of Lignin Nanoparticles (LNPs)

The first stage of this thesis consisted in the production of LNPs from wheat straw, that was composed with several steps.

First it was required to extract the lignin from the biomass using a pre-treatment, the Organosolv using a mixture of ethanol and water as solvent. After successfully remove lignin from the biomass, it was performed a step of precipitation using water as an anti-solvent, producing a solution with LNPs, dissolved lignin, ethanol, water and some impurities.

Finally, in order to purify the nanoparticles, it was used a separation process, diafiltration, with 4 modules of membranes in parallel. At the end of this operation it was obtained a suspension with LNPs and water, the CS.

3.2.1.1. Extraction Process, Organosolv pre-treatment

As it was mentioned before, the pre-treatment used to extract the lignin was the Organosolv pre-treatment. The pre-treatment was performed in a 1 L stirred autoclave (*Zirbus, High Pressure Autoclave HAD 9/16*, Bad Grund, Germany) and the procedure can be described by the following steps:

- 1) The biomass was analysed in order to find out the % of dry mass, through an equipment (*Sartorius*, Germany) that heats up the sample to 120°C and calculates the % of dry mass by the difference on the weight of the sample before and after heating.
- 2) A mixture of 40 g of biomass and 440 g of an aqueous solution of 60 wt % ethanol was made, considering the water in the biomass.
- 3) The mixture was inserted into the autoclave and the extraction was performed at a maximum temperature of 180°C and pressure around 17 bar. During the process, the reactor was controlled with the help of a software *LabView*, that is connected to the sensors of the reactor allowing the operator to check the operational conditions making sure that the set conditions are not exceeded. The heating of the reactor was performed by an external jacket, that in the beginning was set to 220°C and once the 180°C inside the reactor are reached, it was set to 190°C. After 1 hour, the reaction was complete, and the reactor was cooled down with the help of cooling water system.
- 4) The product was removed and placed in a hydraulic press (*HAPA-Press HPH 2.5*, Achern, Germany) at 200 bar in order to separate the liquid fraction from the solid fraction.
- 5) The liquid recovered was centrifuged at 14000 rpm for 20 minutes to remove the remaining solids.
- 6) The final liquid fraction was stored in the fridge (each reaction produced \cong 400 mL of liquid fraction in the end).
- 7) Each extraction was done by repeating step 1 to 6, obtaining approximately 13 L of extract from 33 extractions.

This procedure and operation conditions were chosen based on previous experiments. [20]

The autoclave, press and centrifuge used in the process are shown in the next figures.

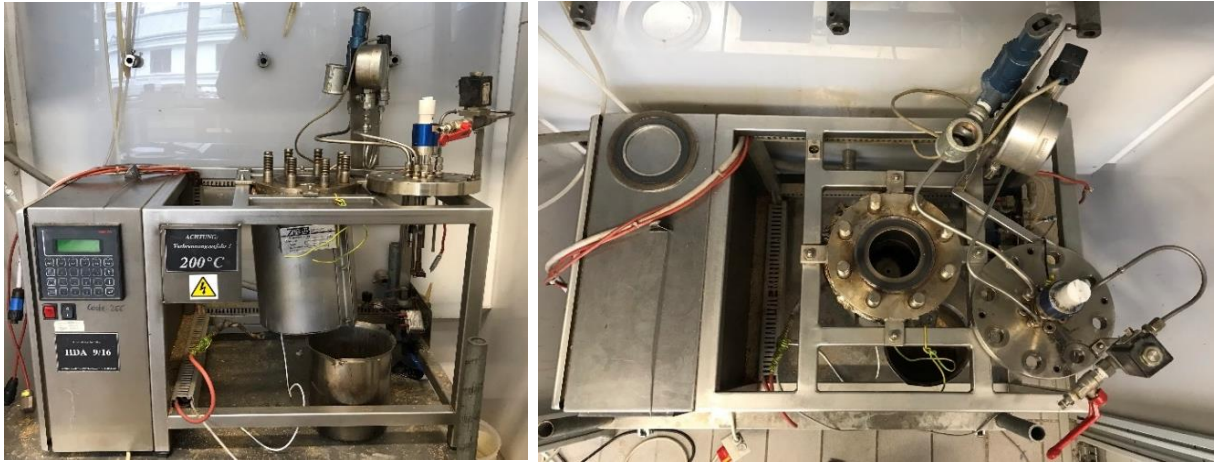


Figure 11. Representation of the autoclave used in the extraction process.



Figure 12. Representation of the press and centrifuge used in the extraction process.

Like it was mentioned above, the operation conditions were controlled by a software and with that it was possible to produce a graphic like the next one.

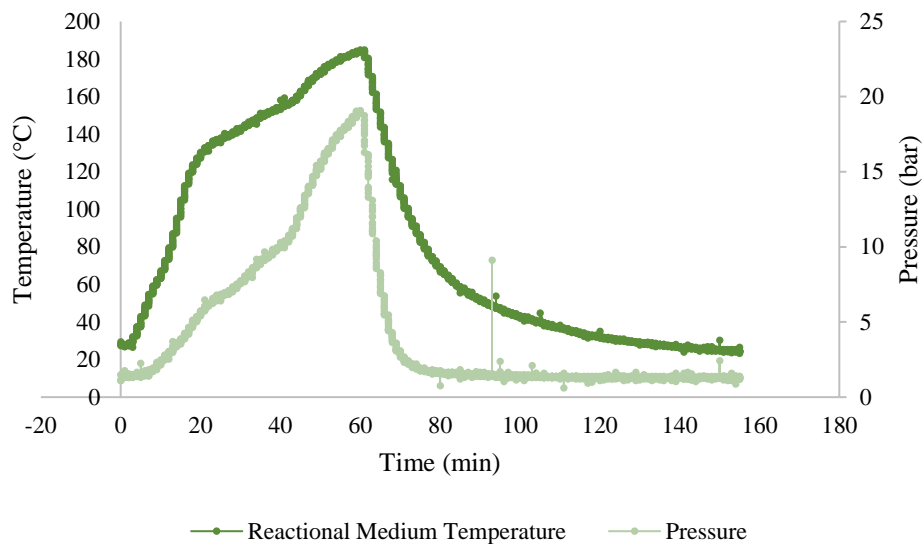


Figure 13. Operation conditions for one extraction of wheat straw.

Each extraction was performed with the same operation conditions. Therefore, all the graphics look the same and like the one from Figure 13 for all 33 extractions. The product of each extraction was stored at first in glass vessels of 1 L, like the one in Figure 14 and afterwards it was stored in cannisters of 10 L.



Figure 14. Vessel used for storage of extractions.

After the extraction, the wheat straw suffered physical changes and that can be seen in Figure 15.



Figure 15. *Left: vessel containing wheat straw before extraction; Right: vessel containing wheat straw dried after extraction.*

Comparing the content in each vessel, it is possible to see that with the extraction process the wheat straw turns darker due to the lack of lignin and hemicellulose, since the Organosolv pre-treatment is known to dissolve lignin and hemicellulose, while cellulose remains as a solid. After the Organosolv pre-treatment, lignin was the component to retrieve from the liquid fraction, meaning that the following steps were crucial. [20]

3.2.2.3. Precipitation of Lignin Nanoparticles (LNPs)

From the previous step, the product obtained was a solution of lignin, ethanol, water and some impurities. For this study, it was important to have nanoparticles, therefore, the solution was submitted to a precipitation, or solvent shifting, using water as an anti-solvent, where the choice of water was made with base in previous experiments. [21] The anti-solvent reduces the solubility of the lignin making the solution saturated and then the particles precipitate.

The precipitation process was performed in the following setup, using a ratio of 1 L of suspension of extract and 5 L of water at 25°C.



Figure 16. Precipitation setup.

There were three vessels, starting from the left: the first one for storage of the extract, the second one for storage of the water and the third one for storage of the precipitate. Each fluid was pumped with a gear pump from *NORD*, into a small cylindrical tube, where they were mixed and the precipitation occurred, obtaining a solution called precipitate with particles with a $\cong 95$ nm radius. It was assumed that half of the lignin in the initial suspension precipitated and the other half stayed dissolved in the solvent with base on previous studies. [21]

3.2.2.4. Diafiltration of the Precipitate

After the precipitation process, it was necessary to remove the impurities using a process of diafiltration. The setup used for this operation is shown in the figure above.



Figure 17. Setup of the operation of the diafiltration.

This model is *Memcell* from *OSMO Membrane Systems* and allows the construction of a crossflow system with several flat modules in parallel or series. The system was composed of 4 modules containing membranes made from hydrophilic polyethersulfone (PESH), UH030 P with 30 kDa cut-off, from Nadir membrane collection supplied by *Microdyn*. The feeding vessel contained the precipitate and, through a gear pump, from *LIQUIFLO*, was pumped through the membranes and it was separated into two currents:

- The permeate that was the current that went through the membrane and removed the dissolved lignin, ethanol and impurities;
- The retentate that was what not went through the membrane and went back to feed vessel.

The conditions of operation used were 20 mL/min and a value of pressure between 2 and 4 bar. After some time of operation, each membrane was regenerated with an aqueous solution of 50 wt % ethanol, to be possible to clean the particles clogging the membranes. The regeneration was supposed to improve the membrane flux, however, this did not happen, because the membranes used for the filtration process were already used ones that already contained some particles attached to them that were clogging the flow.

The diafiltration was performed by filtrating the solution through the modules of membranes and adding water to the vessel, for each litre of permeate removed a litre of water was added. This decreased the concentration of lignin in the solution allowing an increase in the flow through the membrane, since the particles passing through the membrane were less.

To control the process, the concentration of lignin in the permeate through time was measured using an UV spectrophotometer, *UV-1800* from *SHIMADZU* collecting the data with the help of a program called *UVProbe 2.62*. In the beginning the concentration in the permeate was about 0.38 g/L and after the diafiltration it was possible to reach a concentration of 0.02 g/L, meaning that it was possible to stop the diafiltration. Through the process, the solution was kept cold using a cold-water bath at 10°C to prevent the formation of sugars.

By the end of this step, there was the formation of the CS composed of mainly water and precipitated lignin in the form of nanoparticles of $\cong 95$ nm. This suspension was the one used to perform the functionalization.

3.2.2. Functionalization of Lignin Nanoparticles (LNPs)

For the functionalization of LNPs, a silane was used with the methacrylate organic functional group (MSPM). The reactions between the LNPs and MSPM were made after determination of the concentration of lignin and the OH groups per gram of lignin in order to determine the amount of reagent necessary. Towards turning the reagent suitable to react with the LNPs, it was necessary to execute a hydrolysis step before the reactions, to promote the formation of silanol (Si-OH) groups.

Through dry matter analysis and ^{31}P -NMR measurement, the following information was obtained:

- Concentration of lignin in the raw extract = 7.2 g/L;
- Concentration of lignin in the CS = 0.42 g/L;
- Concentration of OH groups in lignin = 9.32 mmol/g.

In order to perform the reactions, it was necessary to consider the following information:

- Density of MSPM = 1.045 g/cm³;
- M_w of MSPM = 248.35 g/mol;
- Density of MSPM = 1 g/cm³;
- M_w of water = 18 g/mol.

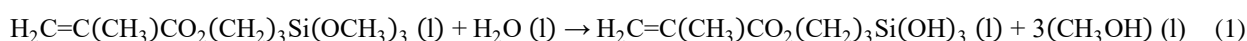
Besides the information mentioned, some assumptions were made:

- Approximately half of the lignin in the raw extract precipitated, half stayed dissolved;
- All OH groups in the LNPs reacts with OH groups in the reagent;
- Excess of water = 2250% (information retrieved from previous experiments).

Conjugating the assumptions and the information collected about the components in the reactions it was possible to determine the quantities to use, but before proceeding, some preliminary reactions were made. The preliminary reactions served as a pre-step to the functionalization to help find the best operations conditions and study the functionalization in small scale.

3.2.2.1. Hydrolysis of the Reagent

The full hydrolysis of the MSPM occurs according to the following reaction:



The amount of reagent necessary was calculated based on the results obtained from the ^{31}P -NMR and dry matter analysis and through stoichiometric calculations it was possible to find out the amount of water to use. In order to study if the dilution factor would affect the reaction between MSPM and LNPs, the hydrolysis was performed with a stoichiometric and excess amount of water at different temperatures and pH's. 6 experiments were performed, with a reaction time of 1 hour and the results are expressed in the following table.

Table 1. Experiments conducted to test the hydrolysis.

| Experiment | pH | Temperature (°C) | State of reaction |
|-------------------|-----------|-------------------------|--------------------------|
| A | 7 | 25 | Turbidity |
| B | 7 | 20 | Turbidity |
| C | 7 | 15 | Turbidity |
| D | 2 | 25 | Turbidity |
| E | 2 | 20 | Turbidity |
| F | 2 | 15 | Clear |

Each experiment represented in Table 1, was conducted using a stoichiometric and excess amount of water and the results were the same for both. From Table 1 it is possible to see that to have a successful hydrolysis it was necessary to resort to a low temperature and pH, despite the amount of water used. Therefore, experiment F was reproduced at least three more times in order to confirm the previous statement and according to the results, with a temperature of approximately 15°C and pH around 2 it is possible to achieve full hydrolysis. The low pH is supported by a study performed on the hydrolysis that concluded that a lower or higher pH increases the rate of hydrolysis of the MSPM. [22]

The hydrolysis was performed in a glass vessel inside a cold-water bath with the help of a magnetic stirrer for 1 hour, until the mixture turned clear. After the reaction was complete, it was stored in the fridge, to prevent the polycondensation.



Figure 18. Demonstration of an unsuccessful (left) and successful (right) hydrolysis of the reagent.

3.2.2.2. Preliminary Reactions

Like it was mentioned before, some preliminary reactions were performed in order to study the functionalization. These reactions were performed with an excess amount of MSPM of 10 times higher towards the OH groups in the CS and with the following conditions:

Table 2. Identification of the solutions used for the preliminary reactions.

| Identification | Experimental Procedure |
|----------------------------------|---|
| I | 5 mL of CS of LNPs obtained from previous steps. |
| Hydrolysis of the reagent | |
| II | Addition of 0.012 mL of MSPM to a stoichiometric amount of acidified water with $\text{pH} \cong 2$ by adding AA and stir the solution for 1 h or until it turns clear. |
| III | Addition of 0.012 mL of reagent to an excess amount (2250%) of acidified water with $\text{pH} \cong 2$ by adding AA and stir the solution for 1 h or until it turns clear. |

Table 3. Identification of the preliminary reactions and experimental conditions.

| Identification | Solutions | Experimental Conditions |
|----------------|-----------|--|
| IIa | I + II | Magnetic stirring of the mixture for 1 h at 25°C and 50°C in a water bath. |
| IIb | I + II | Magnetic stirring of the mixture for 2 h at 25°C and 50°C in a water bath. |
| IIIa | I + III | Magnetic stirring of the mixture for 1 h at 25°C and 50°C in a water bath. |
| IIIb | I + III | Magnetic stirring of the mixture for 2 h at 25°C and 50°C in a water bath. |

By performing these 8 reactions, was possible to retrieve some information regarding the functionalization, more specifically about which parameters to apply in each reaction in a larger scale in order to develop the planification of the scale up of the previous reactions. Each reaction was performed in a small vessel in a water bath to achieve the required temperature.

3.2.2.3. Functionalization

After the preliminary reactions, the planification of the scale up reactions was made and the parameters studied in each reaction were temperature, time of reaction, the amount of MSPM used and the dilution factor (by changing the amount of water used in the hydrolysis). Taking that in consideration, the reactions performed are described in the following tables:

Table 4. Identification of the solutions used for the functionalization reactions.

| Identification | Experimental Procedure |
|----------------|--|
| IV | 200 mg of LNPs (287,439 mL of CS) obtained from previous steps. |
| | Hydrolysis of the reagent |
| V | Addition of 0.148 mL of MSPM to a stoichiometric amount of acidified water with $\text{pH} \cong 2$ by adding AA and stir the solution for 1 h or until it turns clear. |
| VI | Addition of 0.148 mL of reagent to an excess amount of acidified water with $\text{pH} \cong 2$ by adding AA and stir the solution for 1 h or until it turns clear. |
| VII | Addition of 1.476 mL of reagent to a stoichiometric amount of acidified water with $\text{pH} \cong 2$ by adding AA and stir the solution for 1 h or until it turns clear. |
| VIII | Addition of 1.476 mL of reagent to an excess amount of acidified water with $\text{pH} \cong 2$ by adding AA and stir the solution for 1 h or until it turns clear. |

The amount of MSPM used for reactions V and VI was a stoichiometric one towards the amount of OH groups in the CS and VII and VIII were performed with 10 times more than the amount of OH groups.

Table 5. Identification of the solutions used for the functionalization reactions.

| Identification | Solutions | Experimental Conditions |
|----------------|-----------|--|
| Va | IV + V | Magnetic stirring of the mixture for 1 h at 25°C and 50°C in a water bath. |
| Vb | IV + V | Magnetic stirring of the mixture for 3 h at 25°C and 50°C in a water bath. |
| VIa | IV + VI | Magnetic stirring of the mixture for 1 h at 25°C and 50°C in a water bath. |
| VIb | IV + VI | Magnetic stirring of the mixture for 3 h at 25°C and 50°C in a water bath. |
| VIIa | IV + VII | Magnetic stirring of the mixture for 1 h at 25°C and 50°C in a water bath. |
| VIIb | IV + VII | Magnetic stirring of the mixture for 3 h at 25°C and 50°C in a water bath. |
| VIIIa | IV + VIII | Magnetic stirring of the mixture for 1 h at 25°C and 50°C in a water bath. |
| VIIIb | IV + VIII | Magnetic stirring of the mixture for 3 h at 25°C and 50°C in a water bath. |

These 16 reactions were performed in a water bath with magnetic stirring and with similar vessels so the heating characteristics of each reaction would be equal. The setup used is shown in the next figure.

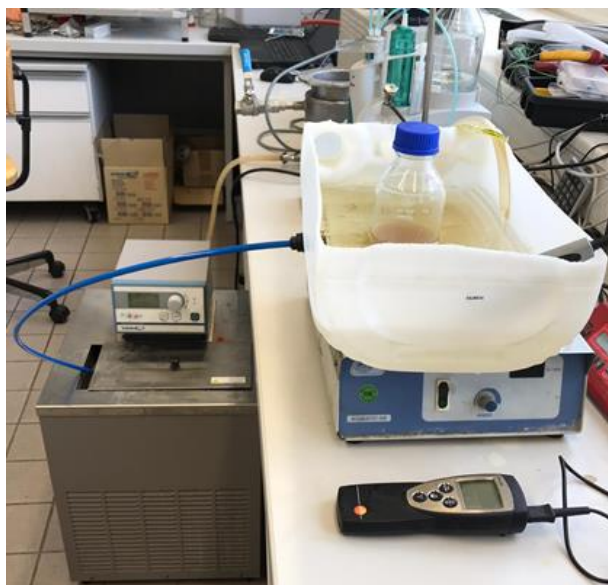


Figure 19. Setup used for the scale up of the functionalization reactions.

The results of each reaction performed are demonstrated in the 5th chapter and properly commented.

4. Characterization Methods

The characterization step was important, towards understanding the modifications done to the LNPs with hydrolysed MSPM. Therefore, there were used three characterization methods that will be briefly described next: Phosphorous-31 Nuclear Magnetic Resonance (P-NMR), Fourier-transformed infrared spectroscopy (FTIR) and Scanning Electron Microscopy (SEM).

4.1. ^{31}P -NMR-spectroscopy

Lignin contains different functional hydroxyl groups such as aliphatic OH, phenolic OH and carboxylic OH. There are several analytical methodologies that give a detailed understanding of the structure of technical lignin's and an efficient one is crucial in the valorisation of it. ^{31}P -NMR-spectroscopy is a technique that enables the quantification of the total OH number and has the advantage of only needing a small sample for a measurement. [23]

Initially, ^{31}P -NMR spectroscopy used to be performed with 2-chloro-1,3,2-dioxaphospholane as the phosphorylating agent, but nowadays it is recommended 2-chloro-4,4,5,5-tetramethyl-1,3,2-dioxaphospholane (TMDP) since it shows better signal preparation. Additional to this, cyclohexanol as internal standard and the relaxation agent chromium(III)acetylacetonate ($\text{Cr}(\text{acac})_3$) are used for the ^{31}P -NMR measurements.

The analysis was performed by dissolving a 30 mg LNPs sample in 200 μL of a dimethylformamide (DMF)/pyridine mixture (1:1, v/v) and shaken with a vortex, since TMDP is moisture sensitive, the solvents used should be anhydrous. Then 50 or 100 μL of a prepared cyclohexanol/ $\text{Cr}(\text{acac})_3$ was added to the lignin sample and homogenized with a vortex for 2-3 minutes. Separately, 400 μL of deuterated chloroform (CDCl_3) and 50 or 100 μL of TMDP were mixed and applied to the lignin sample solution. After a short mixture at room temperature the ^{31}P -NMR-spectrum was measured immediately. The spectra obtained was recorded on a *Bruker Avance 400* NMR 600 MHz spectrometer with an *igated* mode (128 scans, 25 s relaxation time, duration 1 h 50 min).

Using a program called *Mestrenova Version 12.0.0-20080* to analyse all spectra, was possible to determine the OH groups in the lignin sample. First, it was done a manual phase and baseline correction (polynomial fit). Afterwards, all signals observed in the spectra were referenced to the signal at 132.2 ppm and then the integral of the internal standard at 145 ppm was set to 1, while the rest was integrated as usual. The typical integration areas in ^{31}P -NMR for lignin samples are shown in the next Table 6:

Table 6. Integration of the functional groups, adapted from [24, 25].

| Functional group assignment | Chemical Shift Area δ [ppm] |
|-----------------------------|------------------------------------|
| TMDP | 176.0 |
| Aliphatic OH | 145.2 – 150.0 |
| Cyclohexanol (IS) | 144.7 – 145.2 |
| Phenolic OH | 136.5 – 144.5 |
| Carboxylic OH | 133.5 – 136.5 |
| Hydrolysis product of TMDP | 132.2 and 15.9 |
| Not assigned signal | 131.09 – 131.10 |

After the integration, the following equation was applied:

$$\frac{C_{standard} \times V_{standard} \times I_{func.gr.}}{M_{standard} \times I_{standard} \times m_{sample}} = \left[\frac{mmol}{g} \right] \quad (1)$$

Where,

$C_{standard}$ – concentration of cyclohexanol standard [\cong 40 mg/mL];

$V_{standard}$ – volume addition of cyclohexanol standard [50 or 100 μ L];

$I_{func.gr.}$ – integral of corresponding functional group in defined integration area;

$M_{standard}$ – molecular mass of cyclohexanol standard [100.158 g/mol];

$I_{standard}$ – integral of cyclohexanol standard [integral=1];

m_{sample} – lignin sample weight [\cong 30 mg].

The preparation of the LNPs sample was done by two ways: one way was done by taking 80 mL of the CS, washing it with water to remove the small amount of impurities contained in it, freezing it and drying it with the lyophilizer; the other way was to take 80 mL of the CS and dry it as it was.

The lyophilizer used was a *CHRIST ALPHA 1-4 LD* plus from *RIEGER* that is represented in the next figure.



Figure 20. Picture of the lyophilizer used to prepare the samples.

4.2. FTIR-spectroscopy

The Fourier Transformed Infrared Spectroscopy (FTIR) is used to determine the functional groups of a certain sample. [26] The identification of the functional groups was performed by comparing the spectra obtained from each sample with the ones that were found in literature.

Infrared transmission measurements were taken via *VERTEX 70* from *BRUKER* in attenuated total reflectance (ATR) mode in a range between 600 to 4000 cm^{-1} . Each measurement consisted in 16 scans with a resolution of 4 cm^{-1} and at room temperature. The spectra received was analysed with *OPUS 7.0* software in which it was performed the identification of each peaks and the data exportation as .pdf and .txt file format.

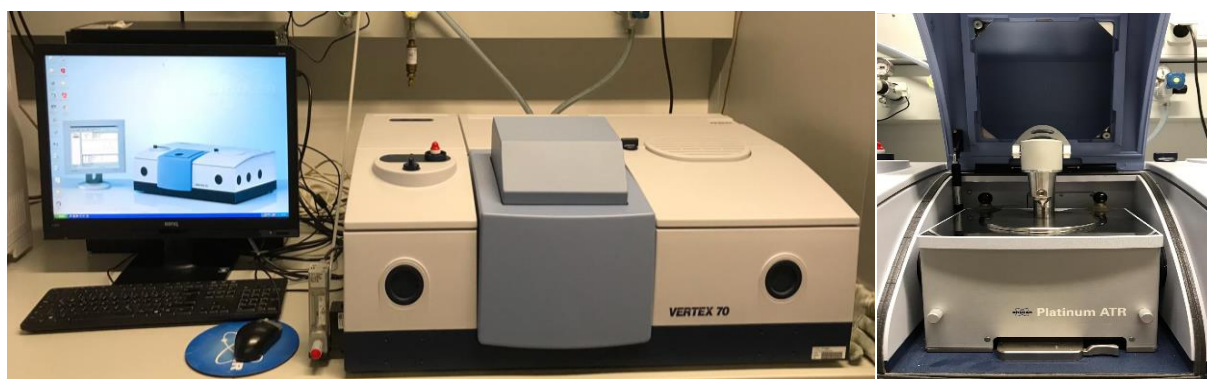


Figure 21. Equipment used for the FTIR measurements.

The measurements were done at a sample of each reaction and CS, that was previously frozen in the freezer and then dried with a lyophilizer. As for the hydrolysed MSPM, it was measured as it was, in its liquid state.

4.3. SEM

In order to see the modifications in the nanoparticles before and after functionalization, it was performed a SEM analysis. The analysis was performed at samples: IIa, IIIa, Va, VIa, VIIa and VIIIa. For this analysis the sample from the product of the reactions was used as it was: a small drop of each was put into a metal plate that was covered with a 4 nm palladium gold layer with the help of sputtering equipment *Quorum Coater Q150TS*. Then the measurement was performed with *EDAX* from *AMETEK*, where several photomicrographs were taken at different magnitudes. For the analysis from the LNPs before functionalization, a sample from the CS was frozen and then dried in the lyophilizer, then it was dispersed in water onto the metal plate being covered with a 4 nm palladium gold layer. The magnification chosen were: 10 000, 100 000 and 200 000 when possible.



Figure 22. Equipment used for the SEM analysis.

5. Results and Discussion

In the following subchapters, the results from each experiment conducted with LNPs will be shown and explained according to the information that was possible to retrieve from it. The results from the characterization performed will also be shown and explained.

5.1. Results from Reactions

5.1.1. Preliminary Reactions

The results obtained from the preliminary reactions mentioned before are shown in the following figures.

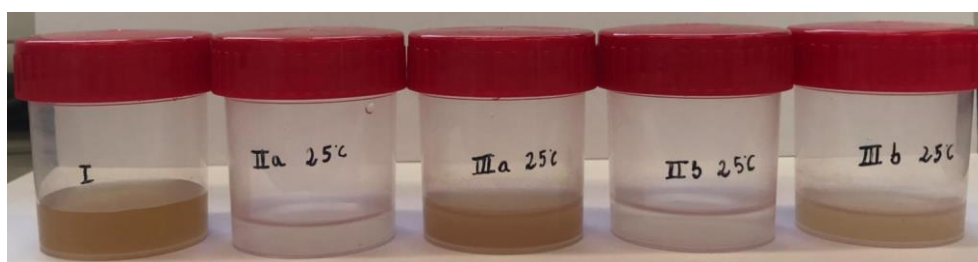


Figure 23. Product from reactions IIa, IIIa, IIb, IIIb at 25°C and solution I.

All of the reactions were performed at 25°C, however, they were performed for different times: 1 hour for IIa and IIIa; 2 hours for IIb and IIIb. Observing the results and comparing it with solution I (sample of CS), it was possible to see that there were physical changes in the MLNPs solution. When applied a solution of hydrolysed reagent with a stoichiometric amount of water it was possible to produce a whitish liquid product, complete different from the initial solution. The same did not happen when an excess amount of water was used for the hydrolysis, not even when the time of reaction was higher.

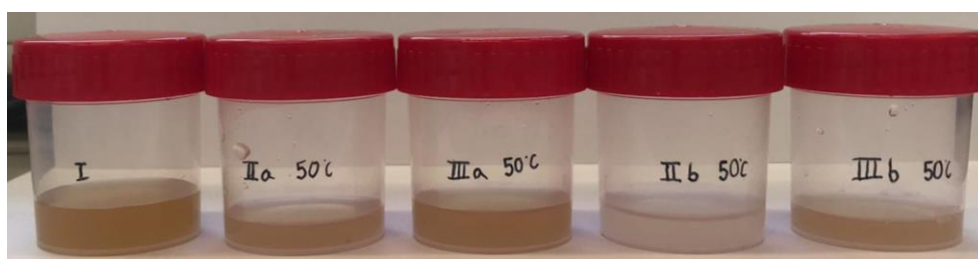


Figure 24. Product from reactions IIa, IIIa, IIb, IIIb at 50°C and solution I.

Regarding the reactions performed at 50°C, the time of reaction also influenced the appearance of the solutions. When the reaction was performed for 1 hour, with a hydrolysed solution where a stoichiometric amount of water was used, the whitish liquid product was not produced, but when the time of reaction increased to 2 hours the desired product was obtained.

These reactions were made, like I mentioned before, to study the functionalization using MSPM in order to favour it by changing several parameters. So, by the end of these reactions, it was possible to determine that the temperature, time of reaction and dilution are important factors to consider.

According to the physical results, when a stoichiometric amount of water was used, the reaction tends to produce a whitish liquid suspension. This alteration in the colour may have happened because of two reasons:

- The hydrolysed MSPM reacted with the LNPs and a consequence of its structural modification was the colour change;
- The hydrolysed MSPM has a high tendency to react with itself and once it was mixed with the CS, covered the nanoparticles turning the whole solution whitish, since the colour of normal mixture of MSPM and water (main component of the CS) is white.

5.1.2. Functionalization

Regarding the functionalization reactions in larger scale, the results from the 16 reactions performed are presented in the following figures along with the CS used as a base.

As mentioned before, according to the previous results, temperature, time of reaction and dilution factor are important factors, but another factor was taken into consideration: the amount of reagent. For half of the reactions performed it was used a ratio of 10 times more MSPM and for the other half it was used a stoichiometric amount.

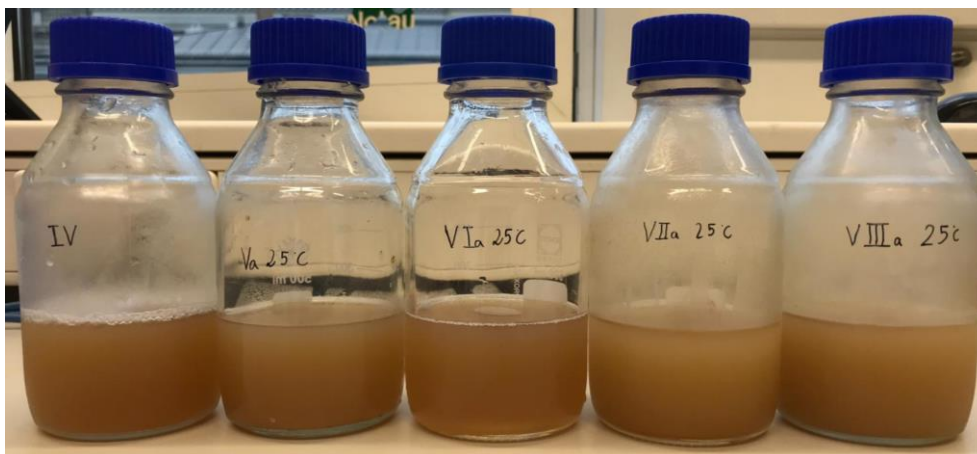


Figure 25. Product from reaction Va, VIa, VIIa and VIIIa at 25°C and solution IV.

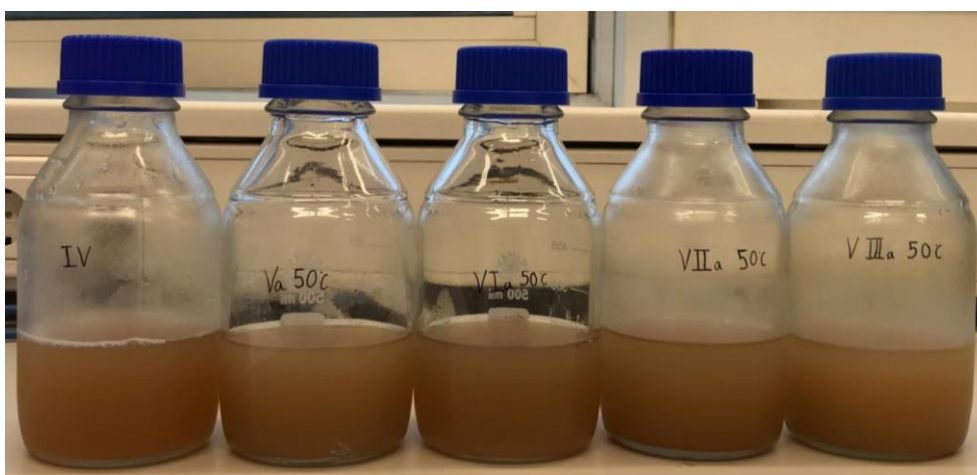


Figure 26. Product from reaction Va, VIa, VIIa and VIIIa at 50°C and solution IV.

All the reactions in Figures 25 and 26, were performed for 1 hour and V and VIa were reacted with stoichiometric amount of MSPM, while VIIa and VIIIa were performed with an amount 10 times higher.

As it is possible to see, in a larger scale there was no production of whitish liquid product like the one produced in the preliminary reactions. However, there were some modifications in the colour, being that the product from each reaction turned lighter.



Figure 27. Product from reaction Vb, VIb, VIIb and VIIIb at 25°C and solution IV.



Figure 28. Product from reactions Vb, VIb, VIIb and VIIIb at 50°C and solution IV.

Regarding the reactions presented in Figures 27 and 28, those were performed for 3 hours and Vb and VIb were made with a stoichiometric amount of MSPM towards the amount of OH groups in the CS, while VIIb and VIIIb were performed with an excess amount of 10 times higher.

Once again, none of the reactions produced the whitish liquid product seen in the preliminary reactions. However, like in the previous reactions, it is possible to see that the product from the reactions was lighter than the CS.

The difference between the results from the preliminary reactions and their scale up, can be attributed to the mixing of the reaction. The mixture between the MSPM and the CS can be considered perfect in the preliminary reactions, since it was a small volume and it was well agitated. As for the scale up reactions, it is possible to see in all the results that there are at least two shades of colours, one lighter and one darker. The volume for these

reactions was higher, meaning that probably the mixing of the reaction was not as effective as it was for smaller volumes.

Once more, some hypotheses are presented for these reactions:

- The hydrolysed MSPM reacted with the LNPs and a consequence of its structural modification was the colour change, however, it did not react with all of it, therefore, there are two type of nanoparticles: modified and unmodified;
- The hydrolysed MSPM has a high tendency to react with itself and once it was mixed with the CS, covered some of the particles turning them white, since the colour of normal mixture of MSPM and water (main component of the CS) is white, while the other ones remain uncovered.
- Part of the hydrolysed MSPM reacted with the LNPs and the other part reacted with itself, leading to a darker part and lighter part, respectively, in the solution.

5.2. Results from Characterization Methods

The following subchapters are redirected to understand the modification that occurs on CS when MSPM was added.

5.2.1. ^{31}P -NMR

Like mentioned before, ^{31}P -NMR was used to measure the amount of OH groups inserted on the CS in order to proceed with the calculations on the amount of MSPM used for the reactions.

According to the study performed by [27] on wheat straw, the total amount of OH groups per gram of lignin extracted by an Organosolv pre-treatment with an aqueous solution of 60% on weight of ethanol at 190°C and measured by ^{31}P -NMR should be around 5.17 mmol. Since the ^{31}P -NMR measurement in the referred study was quite like the one used for this thesis, the value of 5,17 mmol/g_{lignin} served as a reference for the measurements performed.

For each measurement, the important step was the dissolution of the nanoparticles into the mixture of DMF and pyridine, however, the nanoparticles produced in this thesis were not highly soluble into the mixture, meaning only a small part of the sample prepared was dissolved and measured.

The first measurement was performed on the CS as it was, meaning that it was dried and then it was measured according to procedure presented before and the spectra obtained is represented in the following figure.

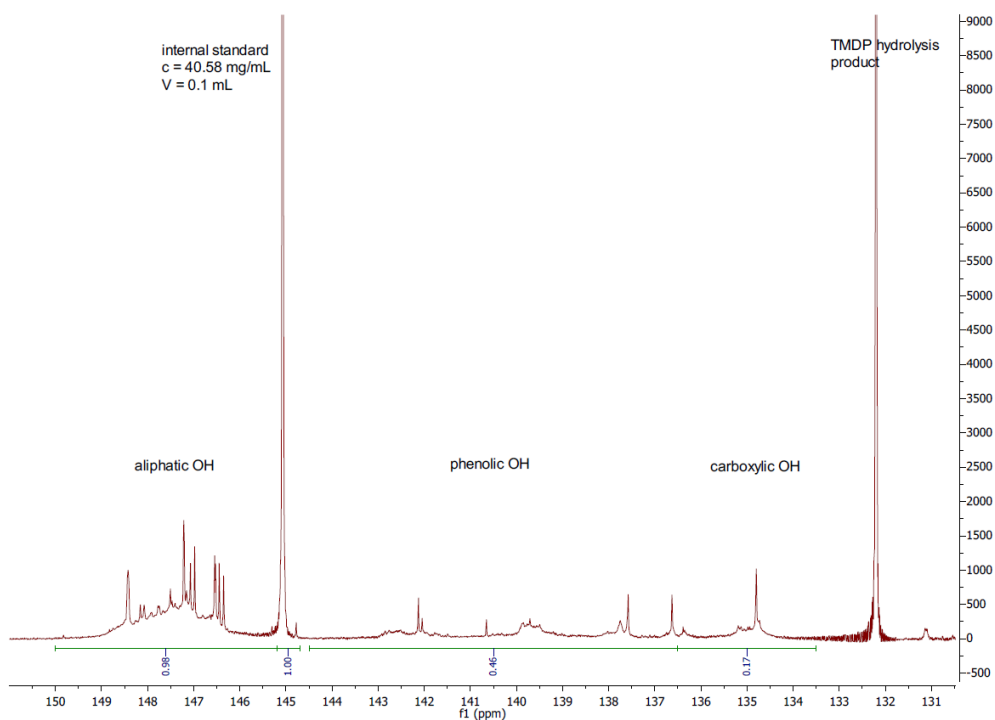


Figure 29. P-NMR results performed at CS.

With the help of the program *Mestrenova*, the values for the respective areas of integration were measured:

- Aliphatic OH = 0.98;
- Phenolic OH = 0.46;
- Carboxylic OH = 0.17.

Conjugating the values and the equation 1 with the data from the standards, the total amount of OH groups per gram of lignin in the CS was 9.32 mmol. This value is higher than the one obtained by [27], due to the OH groups contained in the small portion of impurities that remained in the CS, where sugars were the main component and are the ones that usually have a high number of OH groups, contributing for the high value.

In order to obtain the value of the OH in LNPs without any impurities, the second measurement was performed to a sample of a washed CS with water. The spectra resulted from the second measurement is present in the next figure.

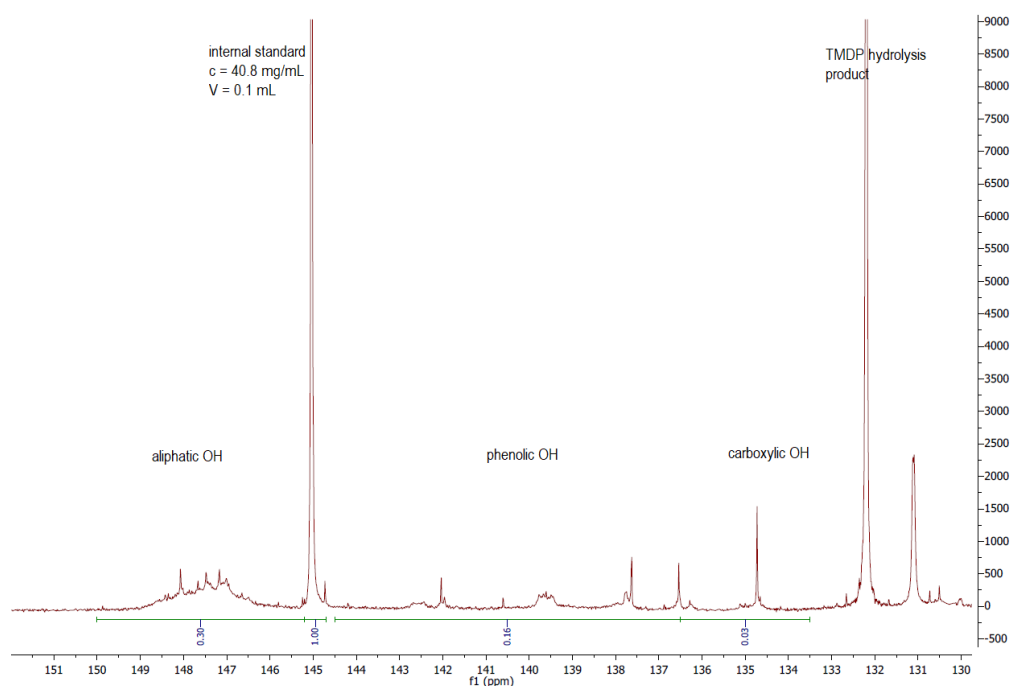


Figure 30. P-NMR results performed at washed CS.

From the second measurement, the values obtained were:

- Aliphatic OH = 0.30;
- Phenolic OH = 0.16;
- Carboxylic OH = 0.03.

Applying once more the equation 1, the result for the total amount of OH groups contained per gram of lignin was 2.84 mmol. As expected, the value was lower than the previous one, since the impurities were all removed, specially the sugars that influence this measurement in a higher portion. It is important to mention that this measurement had an error associated with the weight of the sample used, because it was necessary to use a syringe with a filter before measuring the solution in order to remove some larger particles that did not dissolved. In result of the usage of the filter, the amount of LNPs used for the measurement was smaller than what was weighted, since it was not possible to stipulate the amount retained by the filter. Therefore, the value obtained was considerably smaller than the one obtained in the study performed by [27].

After some research, there were found other values in literature for OH groups per gram of lignin, being those represented in the next table.

Table 7. Values found in literature for the quantification of OH groups in lignin through ^{31}P -NMR.

| Feedstock | Total amount of OH groups (mmol/g_{lignin}) | Reference |
|--|--|------------------|
| European Larch Dust | 9.12 | [28] |
| <i>Miscanthus</i> (milled wood lignin) | 5.79 | [29] |
| <i>Miscanthus</i> (Organosolv lignin) | 4.48 | [29] |
| Wheat Straw | 5.17 | [27] |
| Switchgrass | 7.21 | [30] |
| Triticale | 3.69 | [31] |
| Wheat Straw | 4.05 | [31] |

Through analysing Table 7, it is possible to confirm that the results obtained from the measurements performed are between the range of values reported earlier, taking into consideration the error associated to the second measurement.

The products from the reactions were not analysed by P-NMR, it was not possible due to time and availability of the machine. If the functionalization was successful, it should be expected that the amount of OH groups in the products from the reactions would be around 0. When the functionalization is successful, all OH groups in the hydrolysed MSPM react with the OH groups in the CS.

5.2.2. FTIR-spectroscopy

Performing FTIR to the LNPs before and after modification, can help to understand the chemical modifications performed in its structure and see how the different parameters affected it.

5.2.2.1. Measurement Performed on the Lignin Nanoparticles (LNPs)

In order to have a base line to the product from each reaction, the first measurement was performed on sample of the LNPs from the CS. The correspondent spectrum is showed below.

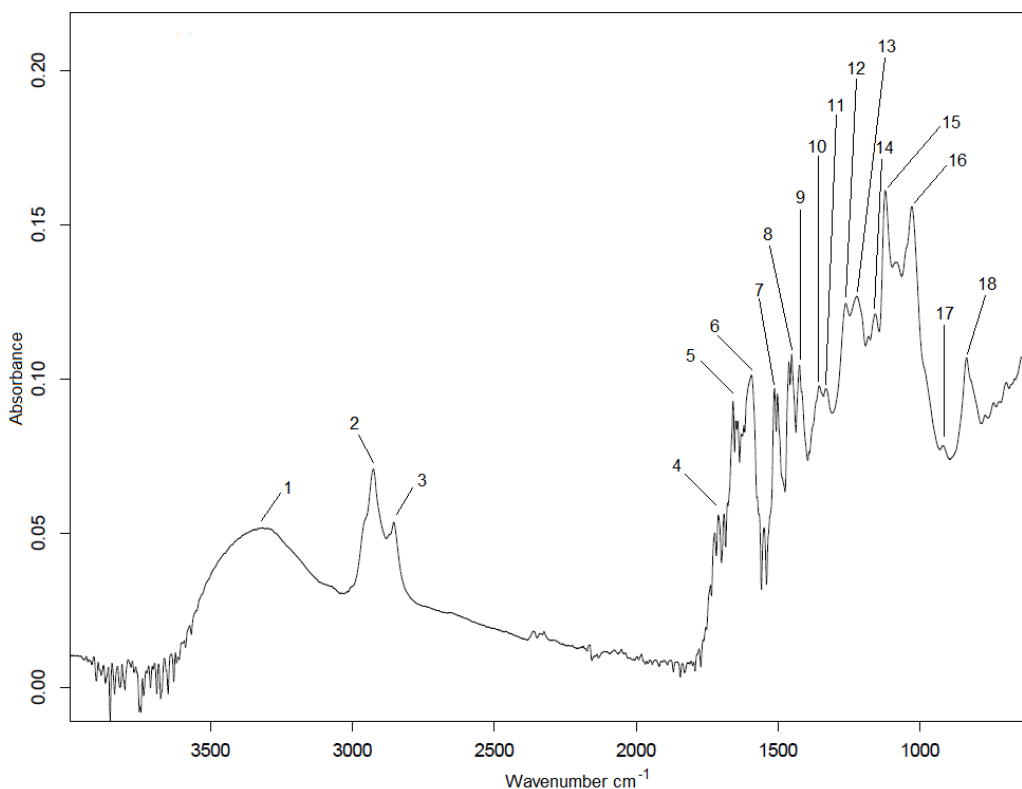


Figure 31. Spectra obtained from the FTIR performed on the LNPs from the CS.

Analysing the spectra, it is possible to identify several peaks. Each one of these peaks matches to a specific bond that can be identified by comparing the correspondent wavenumber with the ones found in literature.

So, in accordance with these previous papers [20, 29–33], the bonds found in the sample of LNPs measured are: a broad band between 3460 cm⁻¹ and 3120 cm⁻¹ that can be attributed to the hydroxyl bond (O-H) stretching, as would be expected, and peaks corresponding to the C-H stretching of methyl and methylene groups (2926 cm⁻¹) and the methyl and methoxyl groups (2860 cm⁻¹). At 1710 cm⁻¹ and 1658 cm⁻¹, it is possible to identify two peaks corresponding to the unconjugated and conjugated C=O stretch, respectively, at different intensities. There are peaks corresponding to aromatic skeletal vibrations (1594 cm⁻¹, 1513 cm⁻¹ and 1424 cm⁻¹) and to asymmetric bending deformation of methyl and methylene groups (1452 cm⁻¹). At 1424 cm⁻¹, 1122 cm⁻¹, 1029 cm⁻¹ appears a C-H in-plane deformation that also appears at 914 cm⁻¹ but out-of-plane. One peak corresponds to C-C bond, at 1220 cm⁻¹. As for C-O bond, there are three bands at 1223 cm⁻¹, 1215 cm⁻¹ and 1029 cm⁻¹ (being this last one a deformation). Wheat straw contains all three major types of monolignols: coniferyl alcohol (G-units), coumaryl alcohol (H-units) and sinapyl alcohol (S-units) being these represented through bands in the spectra. The bands at 1339 cm⁻¹, 1223 cm⁻¹, 1122 cm⁻¹, 836 cm⁻¹ (C-H out-of-plane in position 2 and 6 of S and in all position of H units) and 1153 cm⁻¹ (typical for HGS) are typical for HGS type of lignins. These correspondences are presented in Table 8.

Table 8. Assignments of FTIR measurement on LNPs, adapted from previous studies [20, 29–33].

| Number in Figure 31 | Band (cm ⁻¹) | Assignment |
|---------------------|--------------------------|---|
| 1 | 3316 | O-H Stretch |
| 2 | 2926 | C-H Stretch in methyl and methylene groups |
| 3 | 2860 | C-H Vibration of methyl group of methoxyl groups |
| 4 | 1710 | C=O Stretching, in unconjugated ketones, carbonyls and in ester groups |
| 5 | 1658 | C=O Stretching, in conjugated ρ -substituent carbonyl and carboxyl |
| 6 | 1594 | Aromatic skeletal vibrations and C=O stretch |
| 7 | 1513 | Aromatic skeletal vibrations |
| 8 | 1452 | Asymmetric bending deformation of methyl and methylene groups |
| 9 | 1424 | Aromatic skeletal vibrations combined with C-H in-plane deformation |
| 10 | 1355 | Aliphatic C-H stretch in CH ₃ |
| 11 | 1339 | S ring and G ring condensed |
| 12 | 1223 | C-O of guaiacyl ring and C=O stretch |
| 13 | 1215 | C-C, C-O and C=O stretch |
| 14 | 1153 | Conjugated C=O in ester groups, typical for HGS lignin |
| 15 | 1122 | Aromatic C-H in-plane deformation (typical for S units), C-O deformation in primary alcohols and C=O stretch |
| 16 | 1029 | Aromatic C-H in-plane deformation (G > S), C-O deformation in primary alcohols and C=O stretch (unconjugated) |
| 17 | 914 | C-H out-of-plane, aromatic |
| 18 | 836 | C-H out-of-plane in position 2 and 6 of S and in all position of H units |

5.2.2.2. Measurements Performed on MSPM and Hydrolysed MSPM

Since the functionalization was performed with MSPM, it was performed one measurement on the MSPM as it was received and another one to the MSPM hydrolysed. These measurements can help spot the chemical changes performed in the LNPs after functionalization.

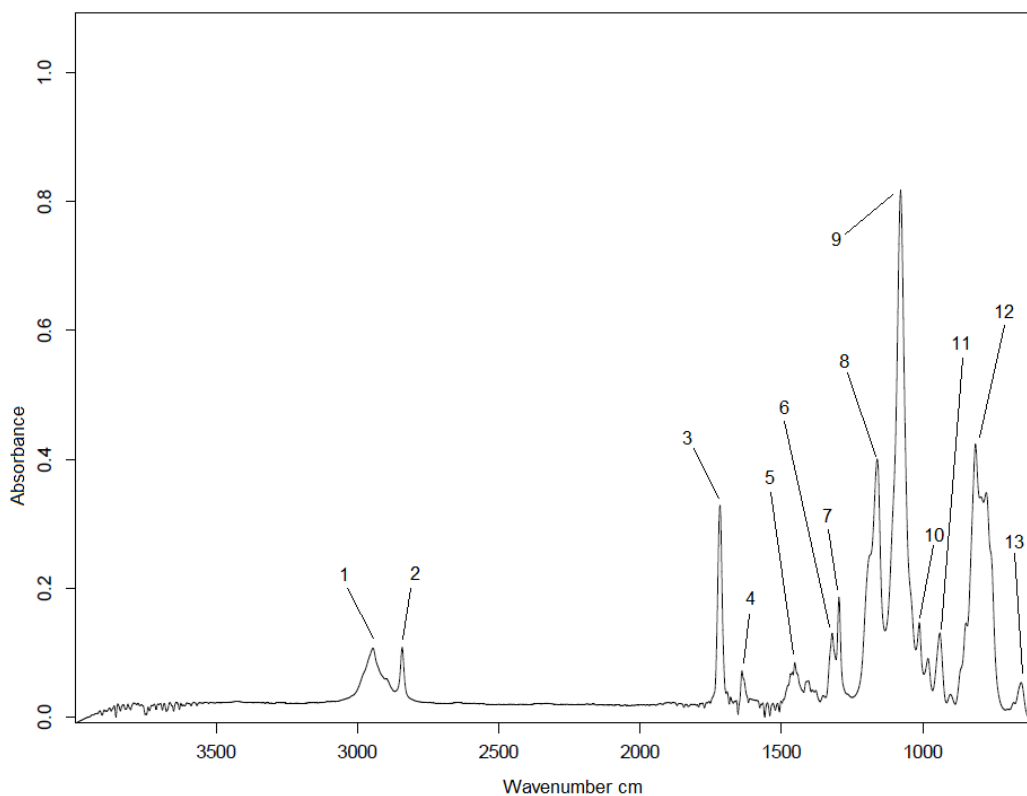


Figure 32. Spectra obtained from the FTIR performed on the MSPM.

By watching the spectra from Figure 32, it is possible to detect peaks on the spectra obtained from the measurement on the MSPM. Once more, using previous studies performed on the analytic method used, the peaks detected were matched with the correspondent bonds.

According to [20, 30, 34–37], the peaks on Figure 32 can be associated to: at 2945 cm^{-1} and 2841 cm^{-1} it is represented C-H stretch in methyl and methylene groups and C-H vibration of methyl group of methoxy, respectively. There is a C=O asymmetric stretch at 1717 cm^{-1} and a C=C stretch at 1639 cm^{-1} . It is possible to find a C-H stretch in CH₃ at 1452 cm^{-1} and then a C-H deformation in the methacrylate group at 1320 cm^{-1} and 1296 cm^{-1} . The band 1161 cm^{-1} corresponds to a Si-O-CH₃ bond, a Si-O bending. Then at 1078 cm^{-1} it is found the C-O-C symmetric stretch and Si-O-C asymmetric stretch. The peaks at 1011 cm^{-1} and 939 cm^{-1} correspond to aromatic skeletal vibrations and the last one to Si-CH₂ asymmetric stretch, that can also be found at 813 cm^{-1} . The last peak, at 652 cm^{-1} , corresponds to the C-O deformation. All correspondences are presented in Table 9.

Table 9. Assignments of FTIR measurement on MSPM, adapted from previous studies [20, 30, 34–37].

| Number in Figure 32 | Band (cm ⁻¹) | Assignment |
|---------------------|--------------------------|--|
| 1 | 2945 | C-H Stretch in methyl and methylene groups |
| 2 | 2841 | C-H vibration of methyl group of methoxy, Si-OCH ₃ |
| 3 | 1717 | C=O Asymmetric stretch |
| 4 | 1639 | C=C Stretch |
| 5 | 1452 | C-H Stretch in CH ₃ |
| 6 | 1320 | C-H deformation in methacrylate group |
| 7 | 1296 | C-H deformation in methacrylate group |
| 8 | 1161 | Si-O-CH ₃ , Si-O bending |
| 9 | 1078 | C-O-C Symmetric stretch, Si-O-CH ₃ asymmetric stretch |
| 10 | 1011 | Aromatic skeletal vibrations |
| 11 | 939 | Aromatic skeletal vibrations and Si-CH ₂ Asymmetric stretch |
| 12 | 813 | Si-CH ₂ Asymmetric stretch |
| 13 | 652 | C-O deformation |

Like it was mentioned, it was performed the hydrolysis of the MSPM and the FTIR measurement to it, so in the following figure it is made a comparison between the measurement of the MSPM and the hydrolysed MSPM.

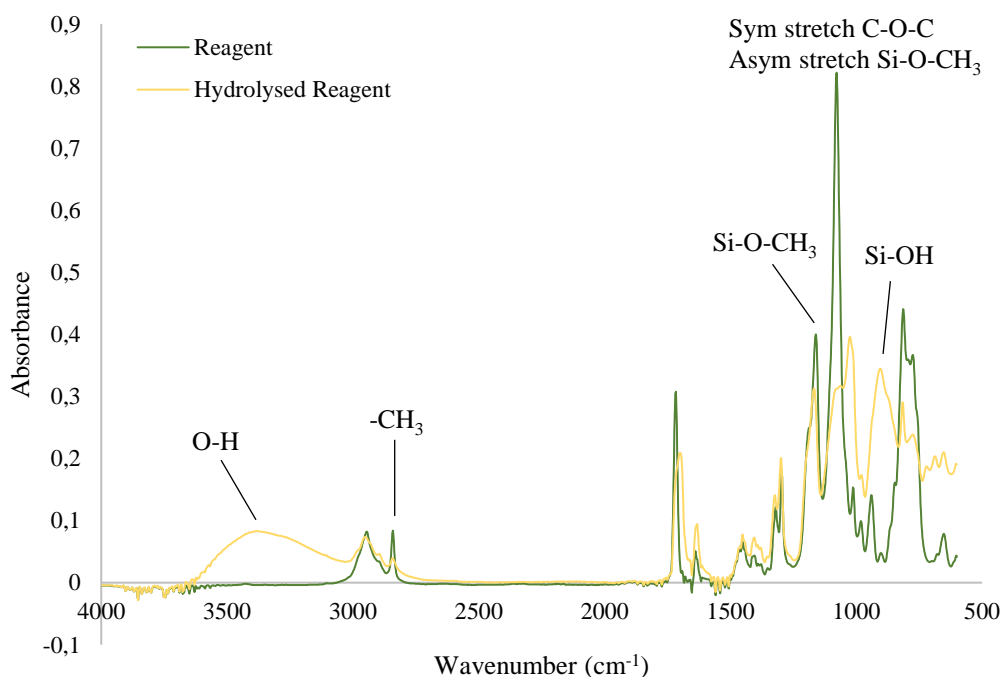


Figure 33. Spectra from the FTIR performed on the reagent and the hydrolysed reagent.

From Figure 33, it is clear that the characteristic bands from MSPM are presented in the hydrolysed reagent, however, there are some bands that have smaller intensity that can mean that the amount of bond correspondent to these specific bands are lesser than the ones found in the MSPM. The bands at 2945 cm^{-1} , 1639 cm^{-1} , 1452 cm^{-1} and 1320 cm^{-1} are the ones that are represented in both samples at the same intensity and correspond to the same bonds presented in Table 9 at the same intensity. The bands at 2841 cm^{-1} , 1717 cm^{-1} , 1296 cm^{-1} , 1161 cm^{-1} , 1078 cm^{-1} , 939 cm^{-1} , 813 cm^{-1} and 652 cm^{-1} are present in both samples, however, in the hydrolysed MSPM sample the intensity is lower, which in the case of 2841 cm^{-1} and 1161 cm^{-1} , it is correspondent to the Si-O-CH₃ and since it has lower intensity it can reflect on the formation of Si-OH bonds. This assumption is supported by the peaks between $960\text{-}840\text{ cm}^{-1}$ correspondents to Si-OH bonds and the appearance of a broad peak at ca. 3300 cm^{-1} ascribed to OH stretching.

So, the main difference between the MSPM and the hydrolysed MSPM in the spectra, are the appearance of peaks associated with the O-H stretch and the Si-OH bonds in the second sample, therefore, the hydrolysis of the MSPM was successful in creating the OH groups necessary for the functionalization of the LNPs.

5.2.2.3. Measurements Performed on the Products of the Functionalization

Since the reactions were performed by adding the hydrolysed MSPM to the CS which contain LNPs, the comparison between the products from each reaction and the LNPs and hydrolysed MSPM is represented in the following figures.

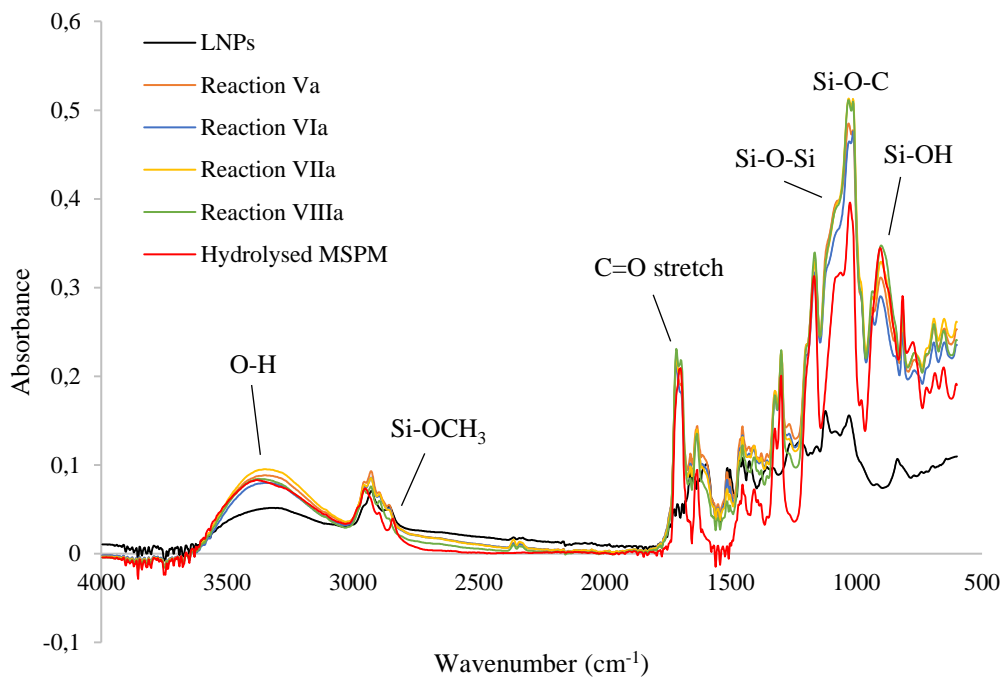


Figure 34. Comparison between the spectra obtained of reactions Va, VIa, VIIa and VIIIa at 25°C and spectra obtained of LNPs and hydrolysed MSPM.

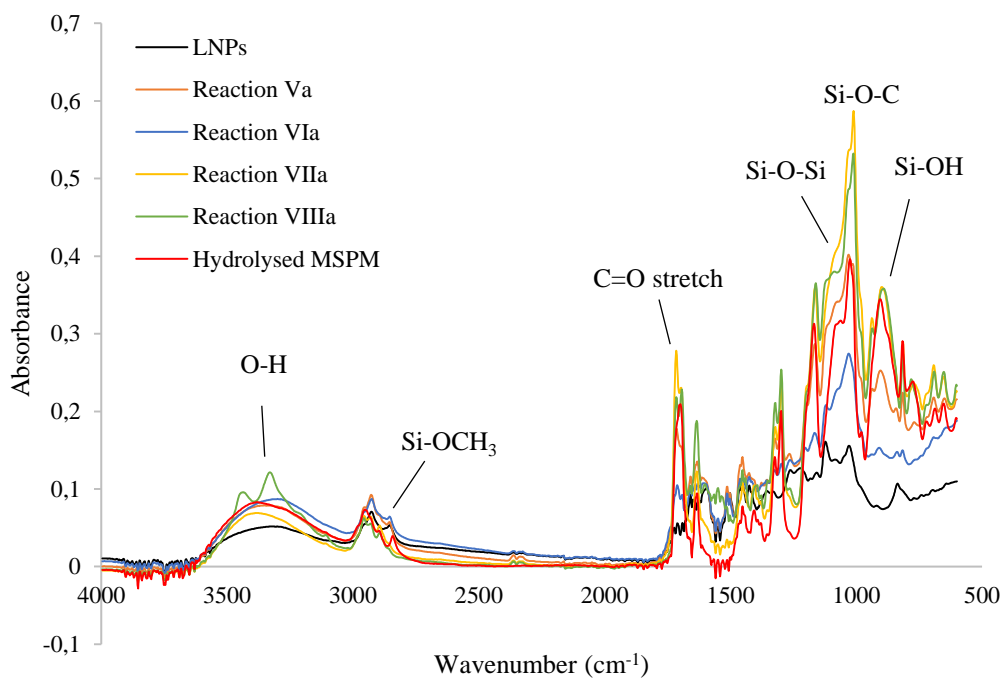


Figure 35. Comparison between the spectra obtained of reactions Va, VIa, VIIa and VIIIa at 50°C and spectra obtained of LNPs and hydrolysed MSPM.

The reactions presented in Figure 34 were performed at 25°C and the ones from Figure 35 are the same ones but performed at 50°C, V and VI stand for when a stoichiometric amount of MSPM is used and VII and VIII when an excess amount of MSPM is used, all of the reactions for 1 h.

Looking at the previous spectra, it is safe to say that each reaction maintained the characteristic bands from lignin with some additional bands derived from the hydrolysed MSPM, with some differences between the reactions.

At a range of 3600 to 3000 cm^{-1} , all of the samples show a wide band correspondent to the O-H bond, which is always with higher intensity than the band from the LNPs, however, the spectra are not normalize. This wide band can derive from the CS of LNPs, which contain water and small residues of ethanol and sugars, etc. and maybe from the hydrolysed MSPM (silanol groups). It is therefore not possible to discern about the origin of these OH groups and conclude about the amount of silanols reacted with the LNPs.

For the reaction products between the hydrolysed MSPM and LNPs, the presence of higher intensity bands at 1030 cm^{-1} and 1010 cm^{-1} , assigned to Si-O-C bonds, might result from the reaction of Si-OH in the hydrolysed MSPM with the OH-lignin. The intensity of these peaks are higher when an excess of MSPM is used, which makes sense and shows that an excess of reagent might favour the functionalization, as expected.

At 1714 cm^{-1} is represented the C=O stretch from the MSPM and between 1055 and 1068 cm^{-1} it is represented the Si-O-Si bond that resulted from the reaction of the MSPM and itself. Also, at 2841 cm^{-1} , is present the Si-OCH₃ that remained after the hydrolysis.

The previous statements regarding the peaks can be applied to all of the reactions represented in the previous spectra. However, when a temperature of 50°C was used, the band representing the O-H bonds has smaller intensity and the band representing the Si-O-C bond has higher intensity compared to the band in the reactions performed at 25°C, which can mean that higher temperatures favour the reaction between the LNPs and the hydrolysed MSPM. There are two exceptions to this, that are the reactions VIa and VIIIa, which possess a higher intensity on the range of the O-H bond, that can be associated to the excess of water used in the hydrolysis of the MSPM. Regarding the band of Si-O-C, once again, the higher temperature favours the formation of this bond.

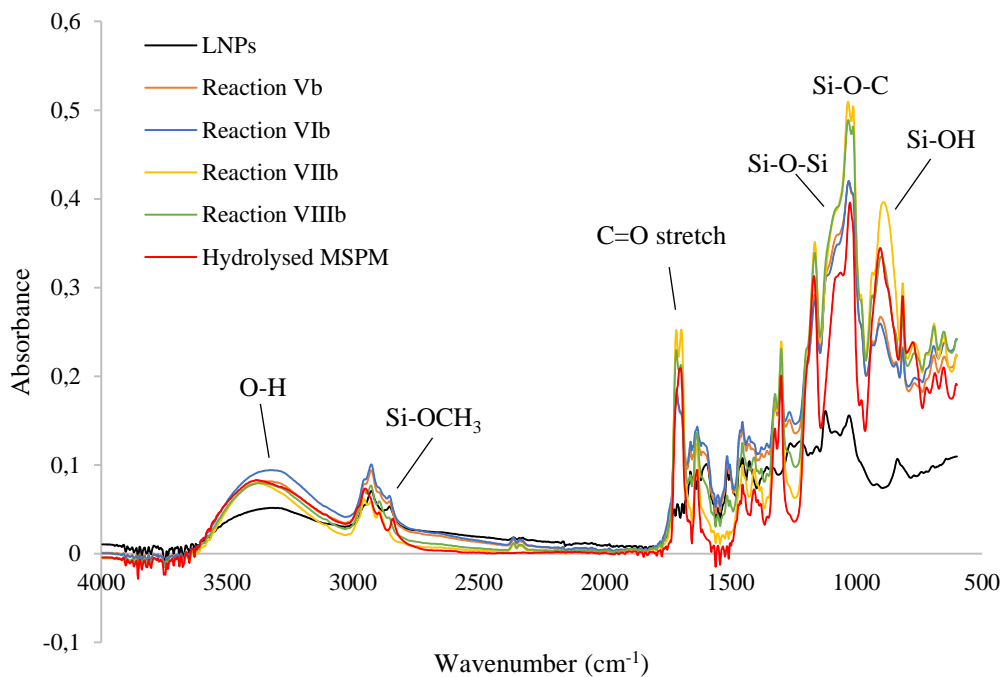


Figure 36. Comparison between the spectra obtained of reactions Vb, VIb, VIIb and VIIIb at 25°C and spectra obtained of LNPs and hydrolysed MSPM.

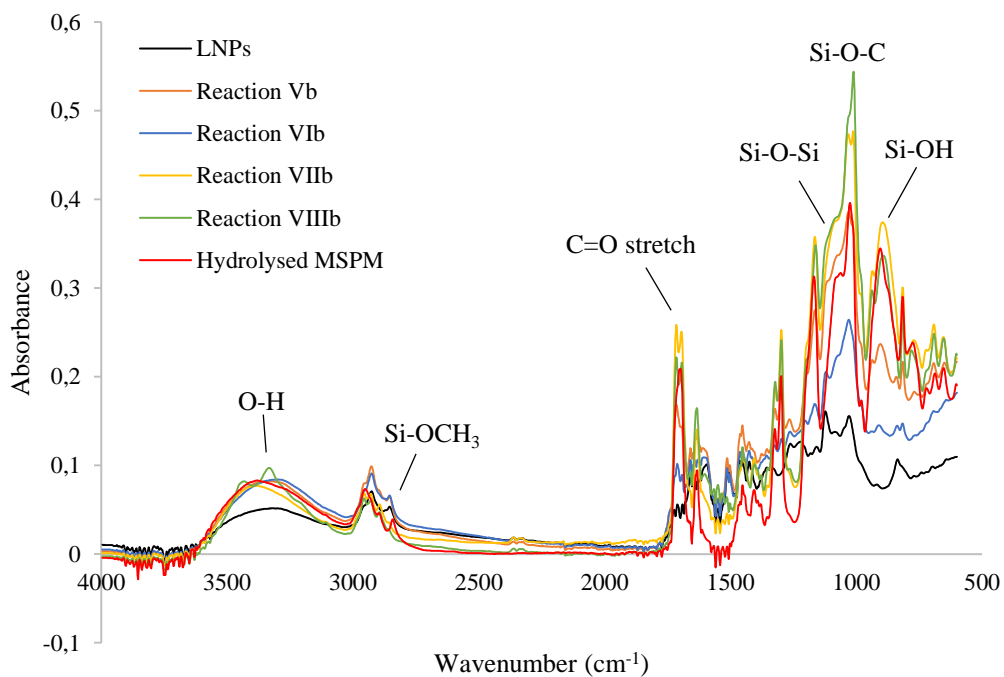


Figure 37. Comparison between the spectra obtained of reactions Vb, VIb, VIIb and VIIIb at 50°C and spectra obtained of LNPs and hydrolysed MSPM.

The spectra from Figures 36 and 37, are from the reactions performed for 3 h with the same conditions of the ones represented in Figures 34 and 35. By comparing the spectra, it is possible to see that they are pretty similar, meaning that the conclusions regarding the reactions performed for 1 h can be applied to the reactions performed for 3 h, as to reference of the peaks found in each spectra. Overall, all the reactions performed maintained the chemical structure of the LNPs with the addition of some of the chemical bonds resulted from the functionalization, as expected.

There is notable a difference between the intensities of both spectra, there is a decrease of the intensities of the peaks mentioned before when the reactions were performed for a longer time. This could mean that the increase of time of reaction does not favour the formation of Si-O-C and, therefore, does not favour the functionalization.

All of the spectra correspondent to each reaction are represented in Annex B with the respective intensities and peak values, serving as a reference towards the conclusions taken from FTIR.

In order to retrieve more information, a quantitative analysis was made on the FTIR results, where it was measured the area of the peaks correspondent to Si-OH and Si-O-C bonds and then the ratio between them. The area of each peak was calculated by a numerical integration, the Newton-Cotes formula. The results are presented in Table 10.

Table 10. Ratio Si-OH/Si-O-C calculated with the data retrieved from FTIR analysis on each reaction.

| Identification | Ratio Si-OH/Si-O-C ($I(980-840 \text{ cm}^{-1}) / I(1070-980 \text{ cm}^{-1})$) |
|-------------------|---|
| Hydrolysed MSPM | 1.235 |
| Va | 0.877 |
| VIa | 0.846 |
| VIIa | 0.880 |
| VIIIa | 0.932 |
| Performed at 25°C | |
| Vb | 0.875 |
| VIb | 0.859 |
| VIIb | 1.067 |
| VIIIb | 0.938 |
| <hr/> | |
| Va | 0.864 |
| VIa | 0.694 |
| VIIa | 0.877 |
| VIIIa | 0.969 |
| Performed at 50°C | |
| Vb | 0.851 |
| VIb | 0.813 |
| VIIb | 1.071 |
| VIIIb | 0.895 |

As is possible to see, there is a remarkable decrease on the ratio of the products towards the hydrolysed MSPM. This might indicate that the reaction of the Si-OH with the OH groups of lignin lead to the formation of Si-O-C bonds, as all the reaction products possess a ratio lower than the hydrolysed MSPM.

The lower the ratio is, higher the area of the Si-O-C peak is, meaning that the functionalization was favoured. From Table 10, the ratios of the reactions performed for 1 hour at higher temperature are lower, which could mean that higher temperatures were more suitable for the reaction that is accordance with the previous assumptions.

Also, when the time of reaction was increased the ratio of those reactions were higher, which leads, once more, to the conclusion that the functionalization does not requires a high amount of time.

5.2.3. SEM

This analytical method has the purpose of detecting physical changes in the LNPs after functionalization.

5.2.3.1. SEM performed on the Lignin Nanoparticles (LNPs)

First it was performed the analysis on the sample of LNPs and then on the MLNPs, all at the same magnitude (100 000) in order to also compare the size of the particles before and after functionalization.

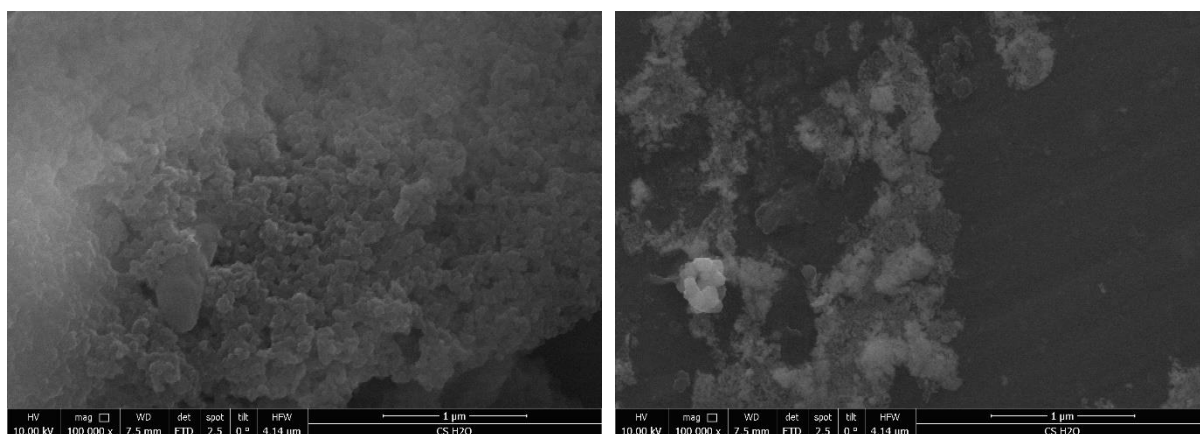


Figure 38. Photomicrographs of LNPs in the CS at 100 000 magnitude.

From SEM analysis, it is possible to see that the LNPs have a slightly round form highly irregular and they tend to agglomerate creating bigger particles. There are single LNPs that can be seen on the photomicrograph

on the right side from Figure 38 and then there are huge agglomerates formed like the ones showed on the photomicrograph on the left in the same figure. Regarding the size of the LNPs, they are on the range of nm according to the magnitude used, but since they tend to agglomerate, they can form particles on the range of μm .

5.2.3.2. SEM performed on the Products of the Functionalization

The following analysis were performed on some of the preliminary reactions and their scale up in order to understand the difference on the colour of the product. Also, they were performed to spot the physical difference between the LNPs and MLNPs.

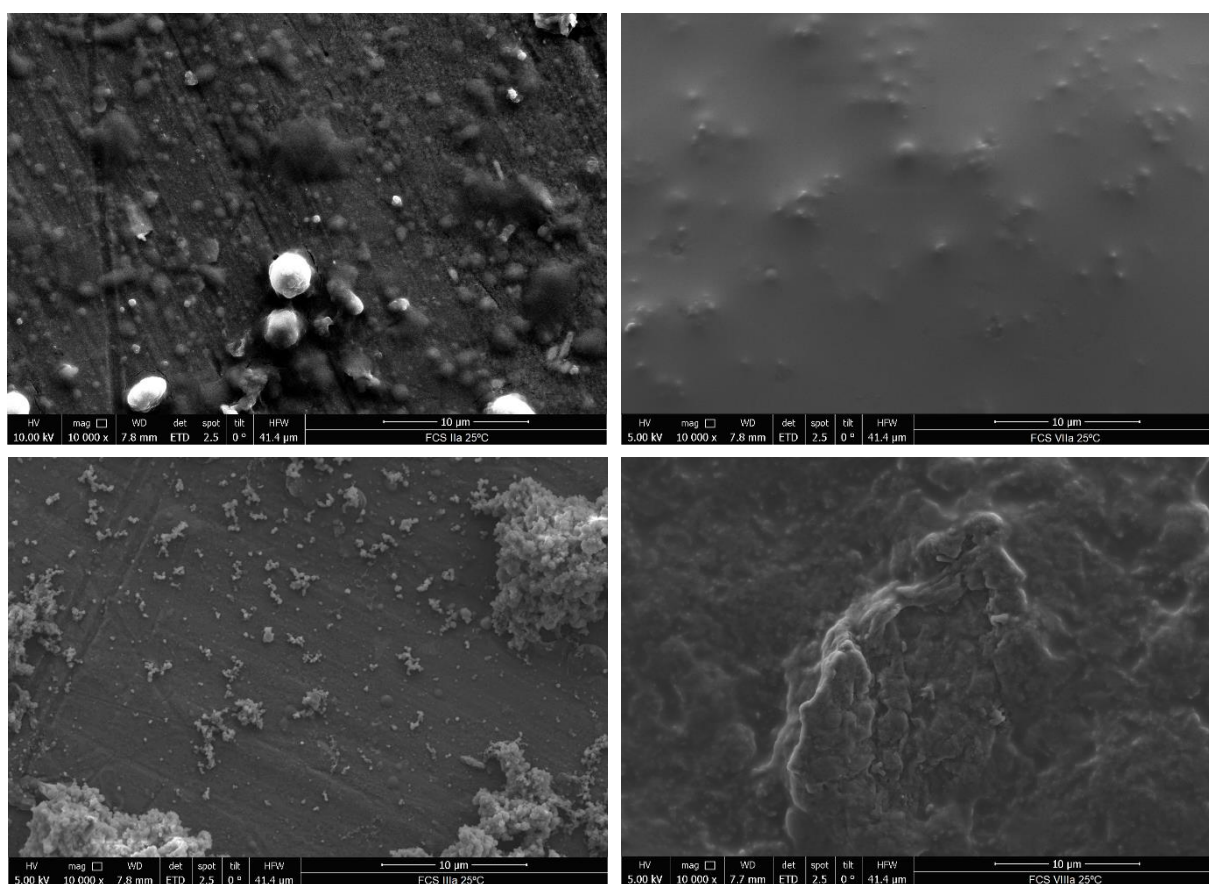


Figure 39. Photomicrographs of the MLNPs for the reactions IIa (top left), IIIa (down left), VIIa (top right) and VIIIa (down right), all at 25°C, for 1 h.

In Figure 39, on the left there are the SEM photomicrographs for the preliminary reactions performed with an excess of MSPM at 25°C and on the right is presented the results for their scale up. The MLNPs from the preliminary reactions on the left side of Figure 39 are more dispersed, smaller and it is possible to find more single MLNPs, also their form is slightly more round and regular. This can be attributed to the perfect mixture achieved

during the reaction, allowing the hydrolysed MSPM react with the LNPs in its fullness. The same does not happen for the scale up, since the amount used was much bigger and the magnetic stirrer was not able to perform a perfect mixture, resulting in the covering of LNPs agglomerates with the reagent, as it is possible to see in the photomicrographs on the right side of Figure 39. Also, the form of the particles in the scale up is highly irregular and there are a lot of agglomerates, being hard to find single MLNPs.

Also, another thing to take into consideration is that, when a higher amount of water was used in the reaction, photomicrographs at the bottom in Figure 39, the particles tend to be more dispersed and the growth of the particles it is not favoured.

Analysis were carried out in order to study the effect of the amount of MSPM used in each reaction.

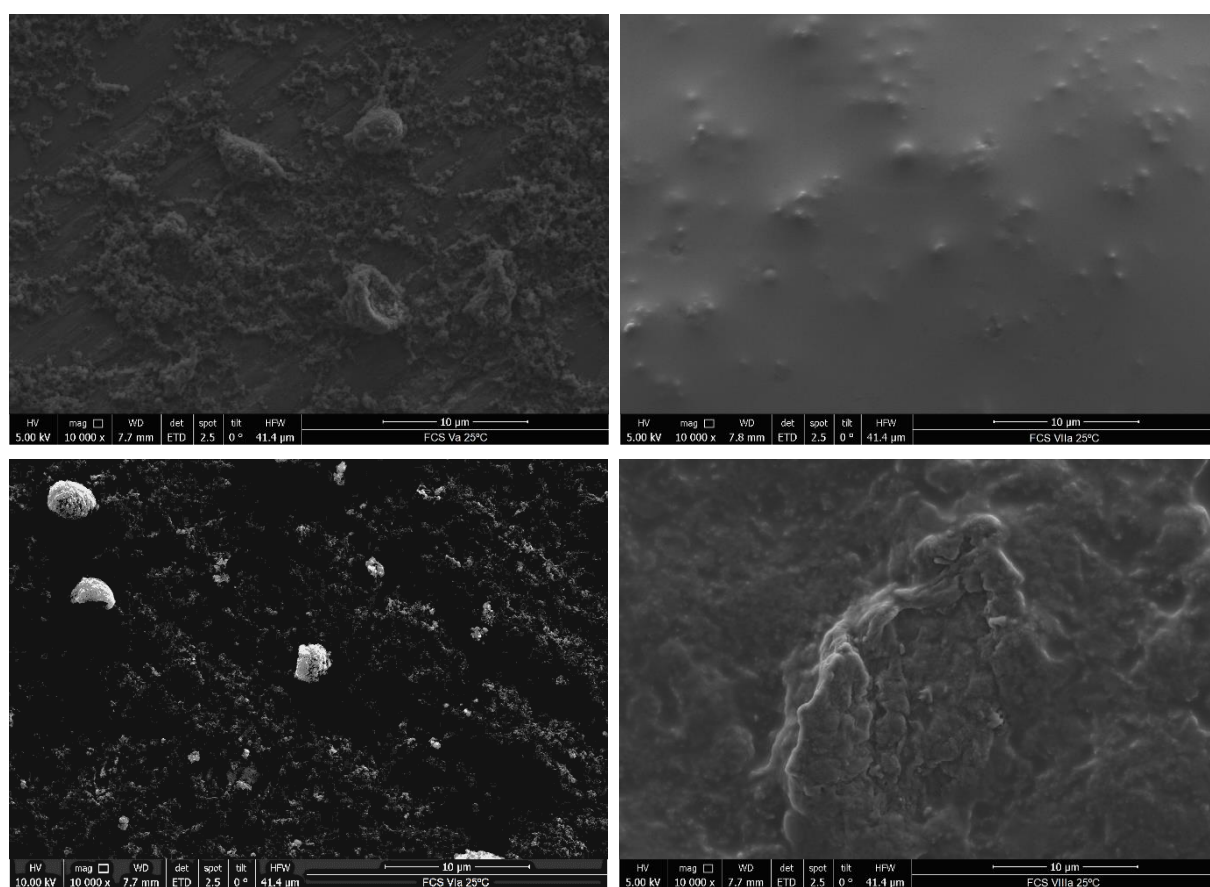


Figure 40. Photomicrographs of the MLNPs for the reactions Va (top left), Vla (down left), Vllla (top right) and Vllla (down right), all at 25°C, for 1 h.

The left side of Figure 40 shows SEM photomicrographs for the reactions performed with a stoichiometric amount of hydrolysed MSPM and the right side shows the ones where an excess of hydrolysed MSPM was used.

Once more, it is possible to see a difference between the size and the form of the particles. When a higher amount of hydrolysed MSPM was used, the particles tend to agglomerate and, therefore, they are bigger and irregular. Also, the particles look like they are covered with the hydrolysed MSPM instead of modified by it. The

use of a stoichiometric amount of MSPM produces rounder particles and with a regular form. Another thing to notice is that the usage of more amount of water (at the bottom in Figure 40) creates a better dispersed suspension.

One other possible conclusion is that when it was used an excess of MSPM, some of it reacted with the lignin and the rest reacted with itself covering the remaining LNPs instead of modifying it, which leads to the photomicrographs on the right side of Figures 39 and 40 and can be supported by the peaks found between 1055-1068 cm^{-1} , correspondent to the Si-O-Si bond. The particle size can also be connected to this parameter, meaning that when the LNPs are almost in their totality modified state, their size remains in the nm range and their form is more regular.

The MLNPs created at higher temperature and longer times of reaction, were observed by SEM, but no significant differences were detected and, therefore, no photomicrographs were taken.

6. Conclusion

The main goal of this project is the functionalization of LNPs by adding vinyl groups to its molecular structure, in order to be able to take part in co-polymerization reactions, replacing monomers derived from fossil fuels in some industrial processes, such as in the production of acrylic fibers or carbon fiber precursors. There are several usages of LNPs ranging from simple polymer blends with improved mechanical properties to promising drug carriers, turning it in a high value product. The properties of LNPs and, consequently, their applications vary according to their feedstock and the extraction process.

The process of lignin extraction used was the Organosolv pre-treatment, which consisted in the usage of aqueous solution of ethanol. Ethanol is an organic solvent, widely available in the market and, in an industrial point of view, cheap and easy to remove from solutions. This pre-treatment was proven to be highly effective in the delignification and in keeping the chemical structure of the lignin, as it was showed by the FTIR performed to the LNPs, since the lignin extracted showed the characteristic bands of lignin, according to literature.

Regarding the production of the LNPs, the solvent shifting process was proven to be effective in producing small particles with a radius of approximately 95 nm and it has a low cost associated, since it uses water as antisolvent. However, it is very slow due to the high content of sugars that clog the pumps used in it. These sugars and other impurities are the downside of the Organosolv pre-treatment, requiring a purification step in order to obtain pure LNPs. By using a diafiltration process, the removal of the impurities was highly effective, but it is quite expensive due to the use of membranes and it was quite slow, since the membranes tend to clog with particles lowering the membrane flux. Overall, the production of LNPs used in the present thesis was quite good having the issue of taking a high amount of time.

The most innovative step of the thesis was the functionalization of the LNPs, which was performed with 3-(trimethoxysilyl)propyl methacrylate. Before the functionalization, the hydrolysis of the reagent was promoted, in order to create the Si-OH groups required to react with the lignin. As far as this study went, the parameters for the hydrolysis of the MSPM had to be optimized to favour hydrolysis and avoid precipitation of the silane. A successful hydrolysis was achieved at a temperature lower than 15°C and with a pH around 2.

Since the functionalization was the main step, it required a small-scale previous study that was performed by doing some preliminary reactions which gave an interesting result as they produced a whitish liquid product. So, to try and reproduce the same results, the parameters studied in the functionalization were time of reaction, amount of MSPM, temperature and dilution factor. The results of the functionalization were analysed by FTIR and SEM. Due to lack of time, ³¹P-NMR was only used to determine the amount of OH groups in the lignin to calculate the amount of hydrolysed MSPM to use in the functionalization step.

One downfall associated with lignin is its solubility that can cause a lot of problems. When performing ³¹P-NMR there were several problems with the dissolution of the LNPs into the standard used solvents, since they were not completely soluble in it. The results obtained were closed to some found in literature, however, they have some error associated to it. The first one has the countability of the OH groups present in the small amount of

impurities and the second measurement has the error associated with the amount of sample lost in the filter, which was not possible to account for.

There was an evidence, by FTIR spectroscopy, of the elimination of part of the Si-O-CH₃ groups and the formation of silanol Si-OH groups with the hydrolysis reaction of MSPM, which was essential for the functionalization process of LNPs with MSPM.

About the results derived from the FTIR on the MLNPs, it is clear that they possess the characteristic bonds found in literature for lignin and MSPM. However, the major finding on the reaction product of the LNPs with the hydrolysed MSPM was a decrease of the ratio Si-OH/Si-O-C (decrease of the ratio I (960-840 cm⁻¹) / I(1070-1000 cm⁻¹)), which might reveal the reaction of the Si-OH with the OH groups of lignin forming Si-O-C bonding's. As for the temperature, when the reaction was performed at 50°C, according to the FTIR results, the reaction between LNPs and the hydrolysed MSPM was favoured and even more when an excess of MSPM was used. In terms of time of reaction, when the reaction was performed for a longer period, the reaction was not favoured, therefore, the functionalization does not require a high amount of time.

Regarding the morphology of the LNPs they are highly irregular, possess a round form and tend to agglomerate. It was concluded that, when performing the functionalization, the stirring is important to achieve a perfect mixture between the hydrolysed MSPM and the LNPs. The reaction product obtained in the preliminary reactions corroborates this finding. By using a higher dilution factor, more water in the reaction, the MLNPs look more dispersed and the agglomeration of the particles is avoided. Also, the use of an excess of MSPM, can lead to the reaction between itself leading to the covering of some of the LNPs.

In conclusion, the functionalization with MSPM was achieved but not in its fullness, leaving some space for optimization. The optimal conditions for a successful functionalization with smaller and regular MLNPS are higher temperatures, good stirring achieving perfect mixture, excess of water and excess of MSPM just to guarantee the reaction of all the OH groups in the lignin.

Work that can be developed in the future:

- 1) Study of the solubility of the LNPs in order to improve ³¹P-NMR results;
- 2) Optimization and further study towards functionalization;
- 3) Further study regarding the applications of these MLNPs in the market, improving their production towards the target application.

References

- [1] Z. Strassberger, S. Tanase, G. Rothenberg, *RSC Adv* **2014**, 4 (48), 25310 – 25318. DOI: 10.1039/C4RA04747H.
- [2] S. Beisl, A. Friedl, A. Miltner, *International journal of molecular sciences* **2017**, 18 (11). DOI: 10.3390/ijms18112367.
- [3] S. Beisl, A. Miltner, A. Friedl, *International journal of molecular sciences* **2017**, 18 (6). DOI: 10.3390/ijms18061244.
- [4] I. Salapa, C. Katsimpouras, E. Topakas, D. Sidiras, *Biomass and Bioenergy* **2017**, 100, 10 – 16. DOI: 10.1016/j.biombioe.2017.03.011.
- [5] W. T. Godbey, *An introduction to biotechnology: The science, technology and medical applications*, Elsevier, Waltham MA **2014**.
- [6] *Lignin and lignans as renewable raw materials* (Eds: F. G. Calvo-Flores), Wiley, Chichester **2016**.
- [7] F. Cherubini, *Energy Conversion and Management* **2010**, 51 (7), 1412 – 1421. DOI: 10.1016/j.enconman.2010.01.015.
- [8] B. Kamm, P. R. Gruber, M. Kamm, *Biorefineries - industrial processes and products: Status quo and future directions*, Wiley-VCH, Weinheim **2006**.
- [9] Jean-Luc Wertz, Magali Deleu, Séverine Coppée and Aurore Richel **2018**.
- [10] Mussato., *Biomass fractionation technologies for a lignocellulosic feedstock based biorefinery*, Elsevier, Amsterdam, Netherlands **2016**.
- [11] R. Kumar, S. Singh, O. V. Singh, *Journal of industrial microbiology & biotechnology* **2008**, 35 (5), 377 – 391. DOI: 10.1007/s10295-008-0327-8.
- [12] P. Figueiredo, K. Lintinen, J. T. Hirvonen, M. A. Kostianen, H. A. Santos, *Progress in Materials Science* **2018**, 93, 233 – 269. DOI: 10.1016/j.pmatsci.2017.12.001.
- [13] Z. Fang, R. L. Smith, *Production of Biofuels and Chemicals from Lignin*, Springer Singapore, Singapore **2016**.
- [14] S.-T. Yang, H. El Enshasy, N. Thongchul, *Bioprocessing technologies in biorefinery for sustainable production of fuels, chemicals, and polymers*, AICHE; John Wiley & Sons Inc, Hoboken New Jersey **2013**.
- [15] S. Beisl, M. Binder, K. Varmuza, A. Miltner, A. Friedl, *ChemEngineering* **2018**, 2 (4), 45. DOI: 10.3390/chemengineering2040045.
- [16] P. Buono, A. Duval, P. Verge, L. Averous, Y. Habibi, *ACS Sustainable Chem. Eng.* **2016**, 2016.

- [17] M. Chauhan, M. Gupta, B. Singh, A. K. Singh, V. K. Gupta, *European Polymer Journal* **2014**, *52*, 32 – 43. DOI: 10.1016/j.eurpolymj.2013.12.016.
- [18] X. He, F. Luzi, W. Yang, Z. Xiao, L. Torre, Y. Xie, D. Puglia, *ACS Sustainable Chem. Eng.* **2018**, *6* (8), 9966 – 9978. DOI: 10.1021/acssuschemeng.8b01202.
- [19] X. Liu, H. Yin, Z. Zhang, B. Diao, J. Li, *Colloids and surfaces. B, Biointerfaces* **2015**, *125*, 230 – 237. DOI: 10.1016/j.colsurfb.2014.11.018.
- [20] S. Beisl, P. Loidolt, A. Miltner, M. Harasek, A. Friedl, *Molecules (Basel, Switzerland)* **2018**, *23* (3). DOI: 10.3390/molecules23030633.
- [21] S. Beisl, P. Loidolt, A. Miltner, A. Friedl, *ChemEngineering* **2018**, *70*.
- [22] A. Tleuova, S. Aidarova, A. Sharipova, N. Bekturganova, M. Schenderlein, D. Grigoriev, *Colloids and Surfaces A: Physicochemical and Engineering Aspects* **2016**, *505*, 18 – 22. DOI: 10.1016/j.colsurfa.2015.10.057.
- [23] M. Balakshin, E. Capanema, *Journal of Wood Chemistry and Technology* **2015**, *35* (3), 220 – 237. DOI: 10.1080/02773813.2014.928328.
- [24] B. Ahvazi, O. Wojciechowicz, T.-M. Ton-That, J. Hawari, *Journal of agricultural and food chemistry* **2011**, *59* (19), 10505 – 10516. DOI: 10.1021/jf202452m.
- [25] Y. Pu, S. Cao, A. J. Ragauskas, *Energy Environ. Sci.* **2011**, *4* (9), 3154. DOI: 10.1039/c1ee01201k.
- [26] B. C. Smith, *Fundamentals of Fourier transform infrared spectroscopy*, 2nd ed., CRC Press, Boca Raton, Fla **2011**.
- [27] W.J.J. Huijgen, G. Telysheva, A. Arshanitsa, R.J.A. Gosselink, P. J. de Wild, *Industrial Crops and Products* **2014**, *59*, 85 – 95. DOI: 10.1016/j.indcrop.2014.05.003.
- [28] M. Hochegger, B. Cottyn-Boitte, L. Cézard, S. Schober, M. Mittelbach, *International Journal of Chemical Engineering* **2019**, *2019* (3), 1 – 10. DOI: 10.1155/2019/1734507.
- [29] R. El Hage, N. Brosse, L. Chrusciel, C. Sanchez, P. Sannigrahi, A. Ragauskas, *Polymer Degradation and Stability* **2009**, *94* (10), 1632 – 1638. DOI: 10.1016/j.polymdegradstab.2009.07.007.
- [30] G. Hu, C. Cateto, Y. Pu, R. Samuel, A. J. Ragauskas, *Energy Fuels* **2012**, *26* (1), 740 – 745. DOI: 10.1021/ef201477p.
- [31] F. Monteil-Rivera, M. Phuong, M. Ye, A. Halasz, J. Hawari, *Industrial Crops and Products* **2013**, *41*, 356 – 364. DOI: 10.1016/j.indcrop.2012.04.049.
- [32] F. Xu, J.-X. Sun, R. Sun, P. Fowler, M. S. Baird, *Industrial Crops and Products* **2006**, *23* (2), 180 – 193. DOI: 10.1016/j.indcrop.2005.05.008.
- [33] L. Yao, C. Chen, C. G. Yoo, X. Meng, M. Li, Y. Pu, A. J. Ragauskas, C. Dong, H. Yang, *ACS Sustainable Chem. Eng.* **2018**, *6* (11), 14767 – 14773. DOI: 10.1021/acssuschemeng.8b03290.

- [34] N. A. Rangel-Vázquez, T. Leal-García, *Journal of the Mexican Chemical Society* **2010**, 2010, 192 – 197.
- [35] R. Salgado-Delgado, A. M. Salgado-Delgado, E. García-Hernández, A. Olarte-Paredes, Z. Vargas-Galarza, V. M. Castaño, *IJERA* **2016**, 2016 / Vol. 6, 4 – 7. DOI: 10.9790/9622.
- [36] G. Socrates, *Infrared and Raman characteristic group frequencies: Tables and charts*, 3rd ed., John Wiley & Sons, Chichester **2001**.
- [37] P. J. Launer, B. Arkles, *Infrared Analysis of Organosilicon Compounds: Spectra-Structure Correlations*, https://www.gelest.com/themencode-pdf-viewer/?file=https://www.gelest.com/wp-content/uploads/5000A_Section1_InfraredAnalysis.pdf **2013**.

Annex A – Block Diagram from the Overall Process

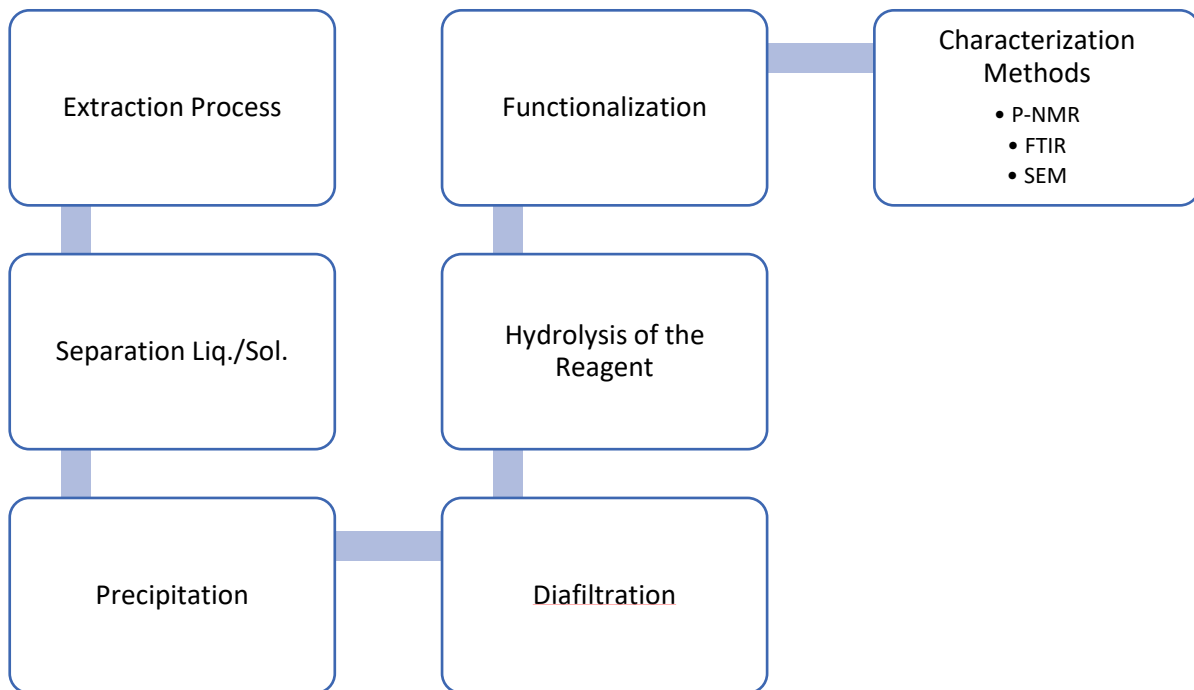


Figure 41. Block diagram from the overall process study in this thesis.

Annex B – Spectrums from FTIR measurements with the respective peaks for each sample

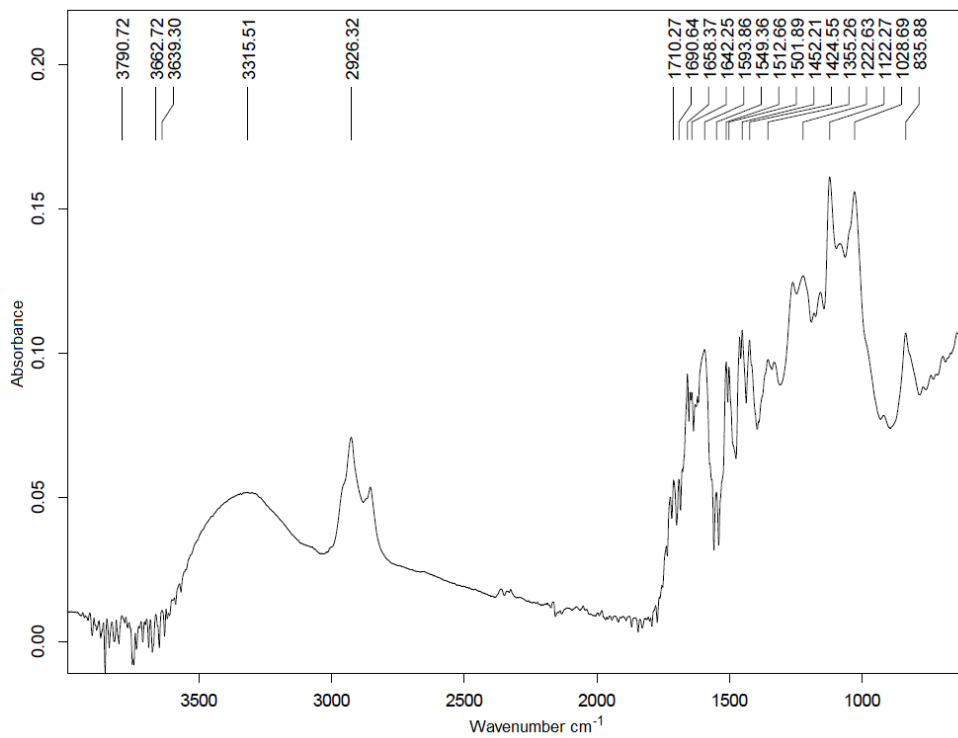


Figure 42. Spectra from FTIR measurement on the LNPs.

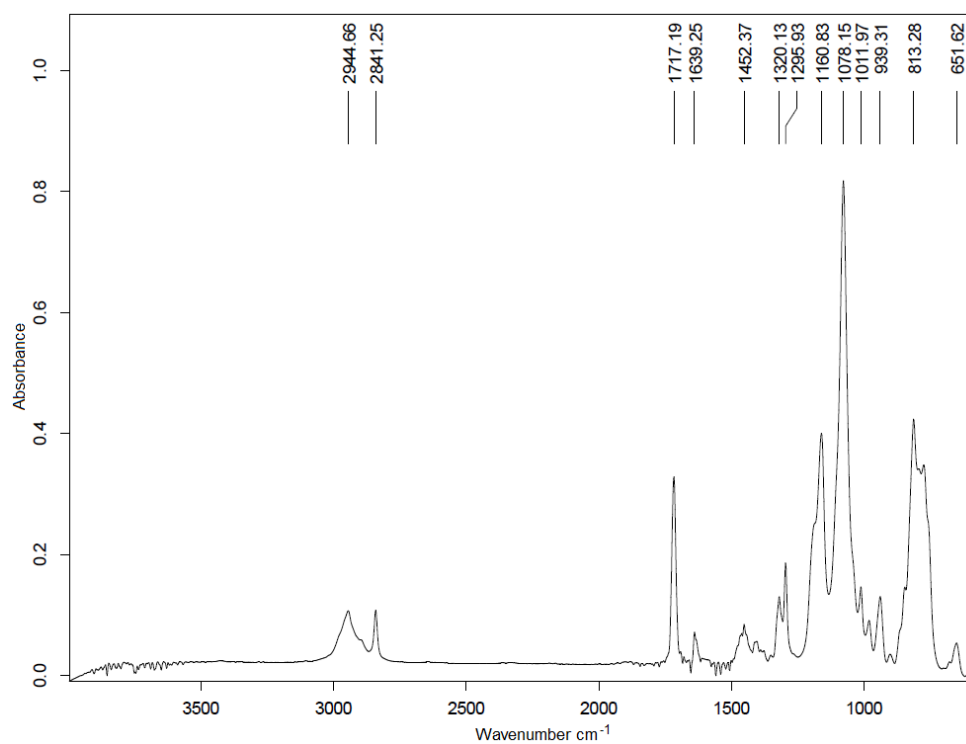


Figure 43. Spectra from FTIR measurement on the MSPM.

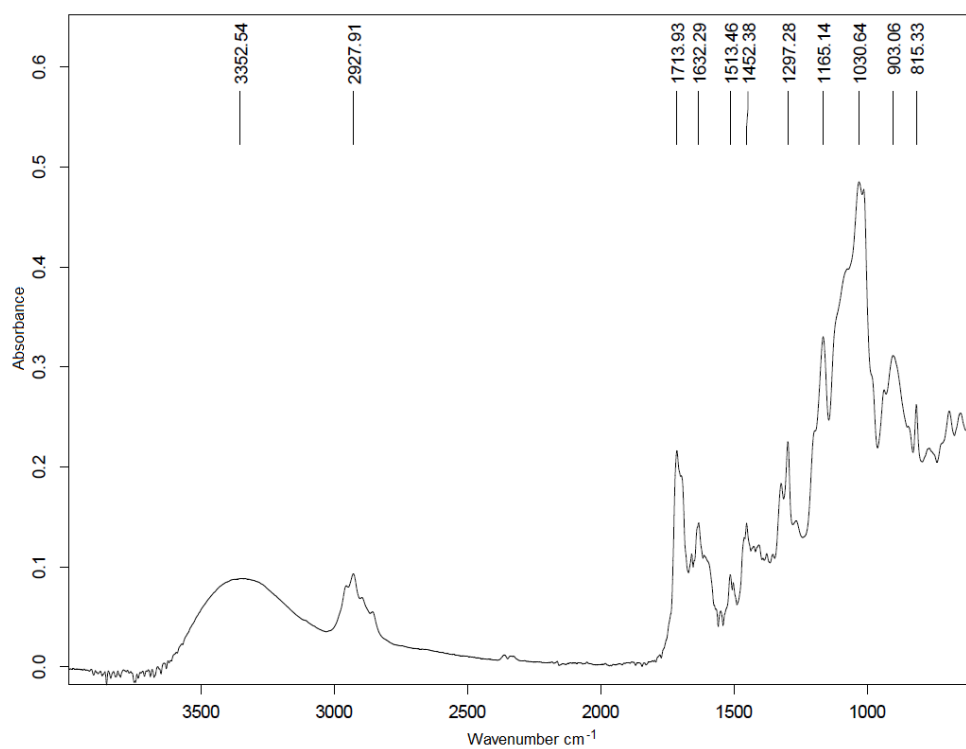


Figure 44. Spectra from FTIR measurement on reaction Va at 25°C.

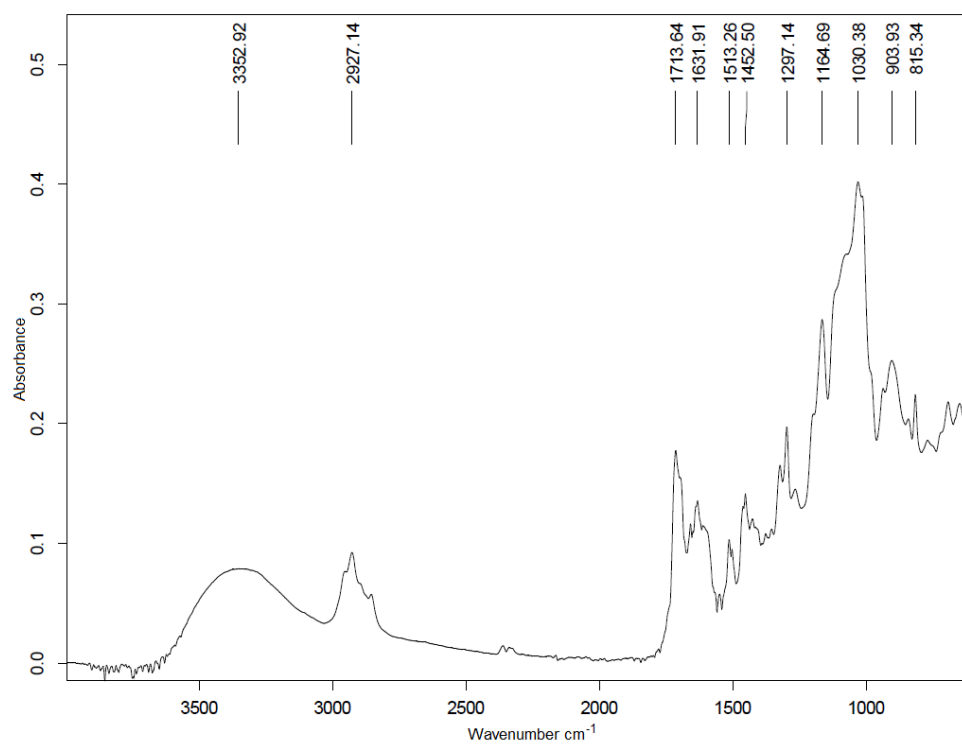


Figure 45. Spectra from FTIR measurement on reaction Va at 50°C.

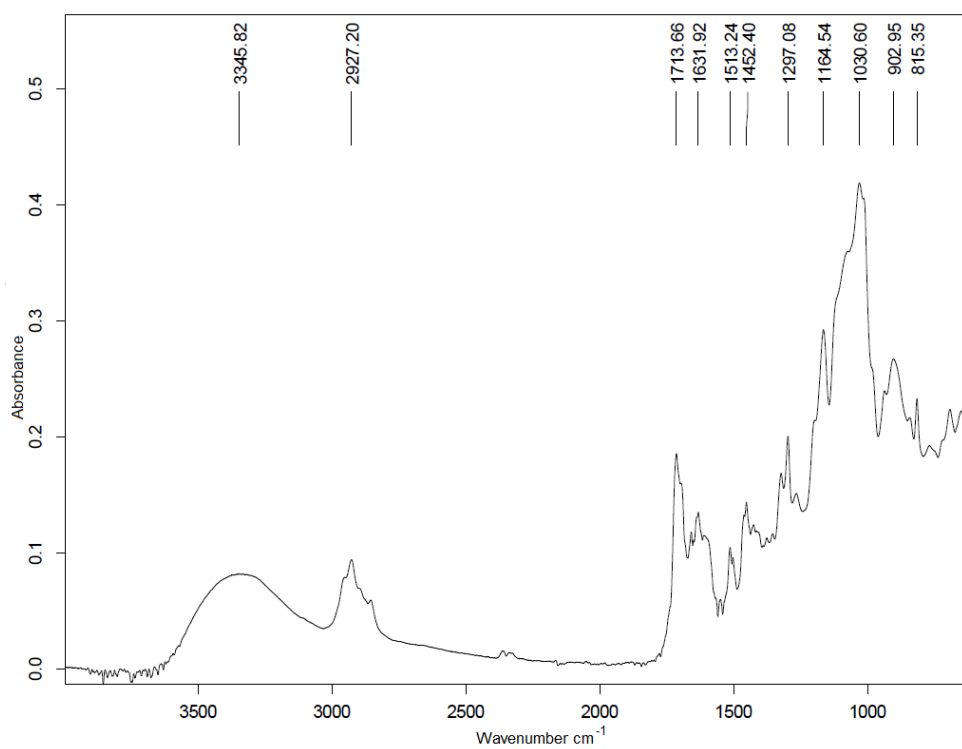


Figure 46. Spectra from FTIR measurement on reaction Vb at 25°C.

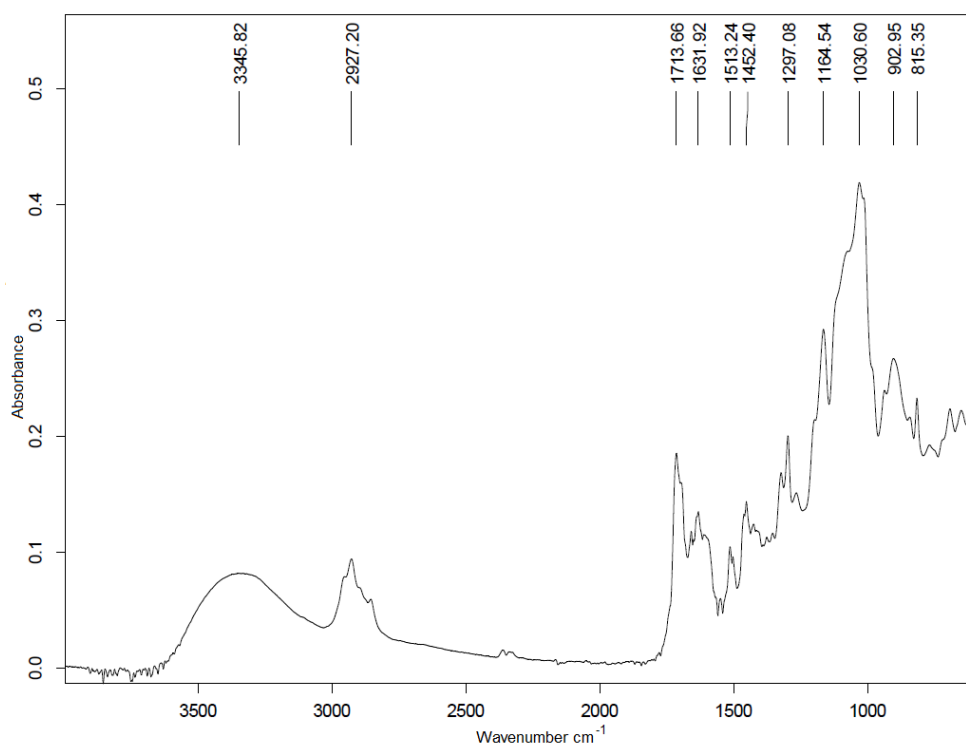


Figure 47. Spectra from FTIR measurement on reaction Vb at 50°C .

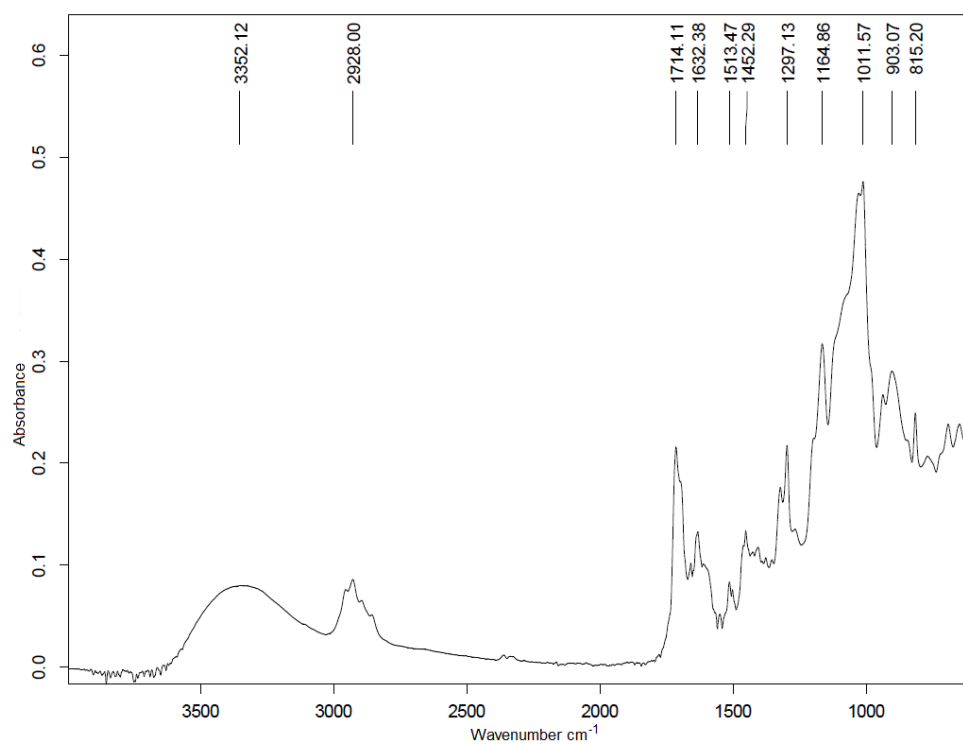


Figure 48. Spectra from FTIR measurement on reaction VIa at 25°C .

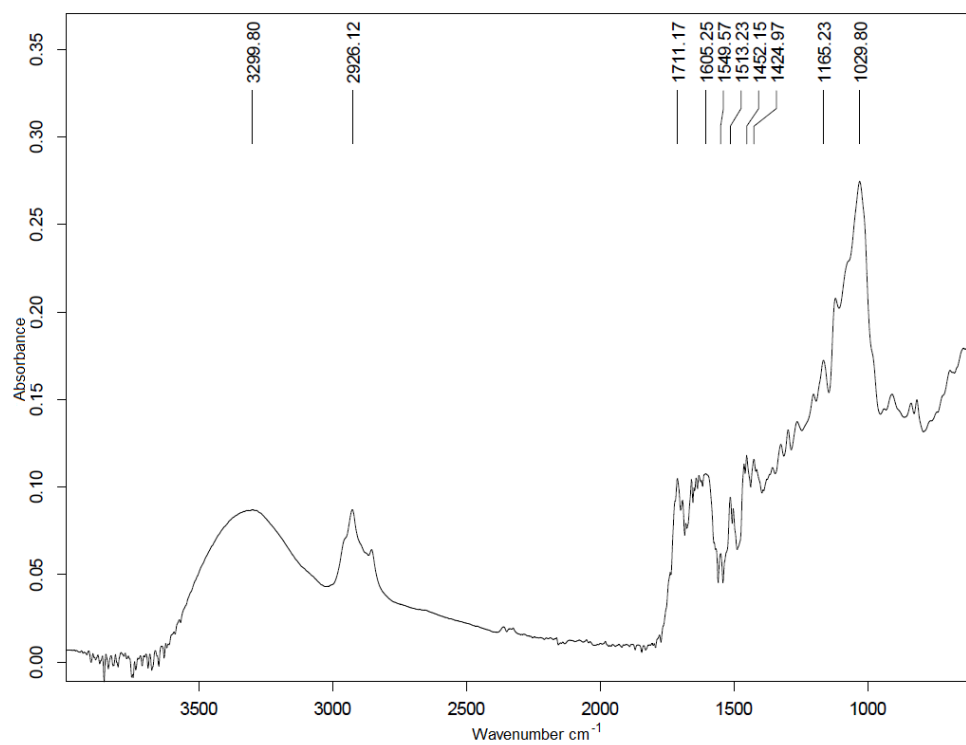


Figure 49. Spectra from FTIR measurement on reaction VIa at 50°C.

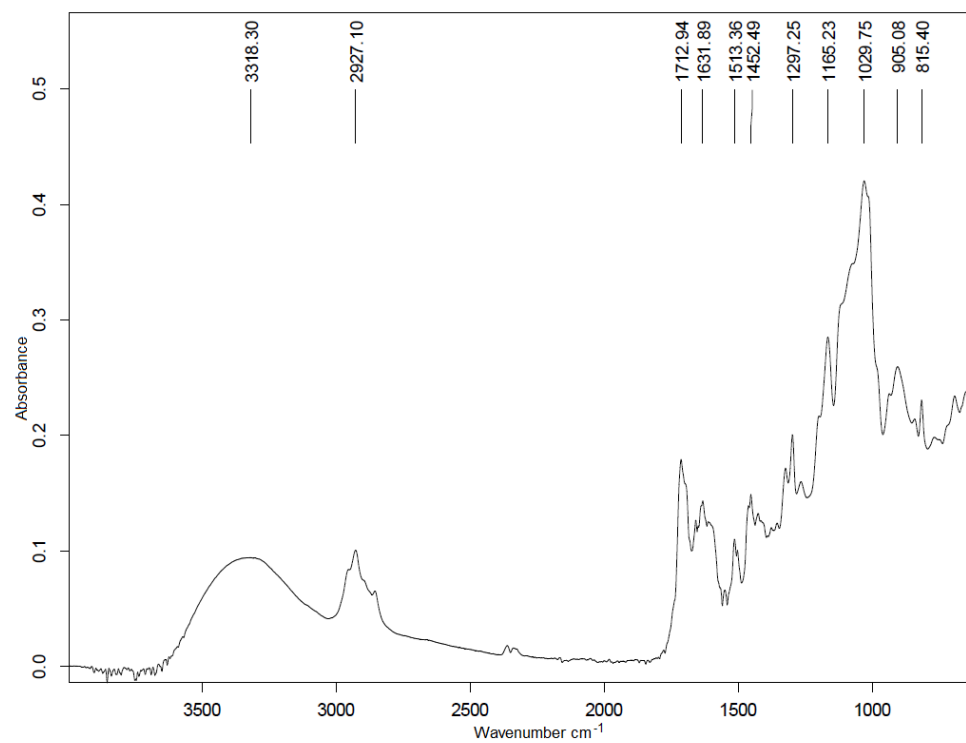


Figure 50. Spectra from FTIR measurement on reaction VIb at 25°C.

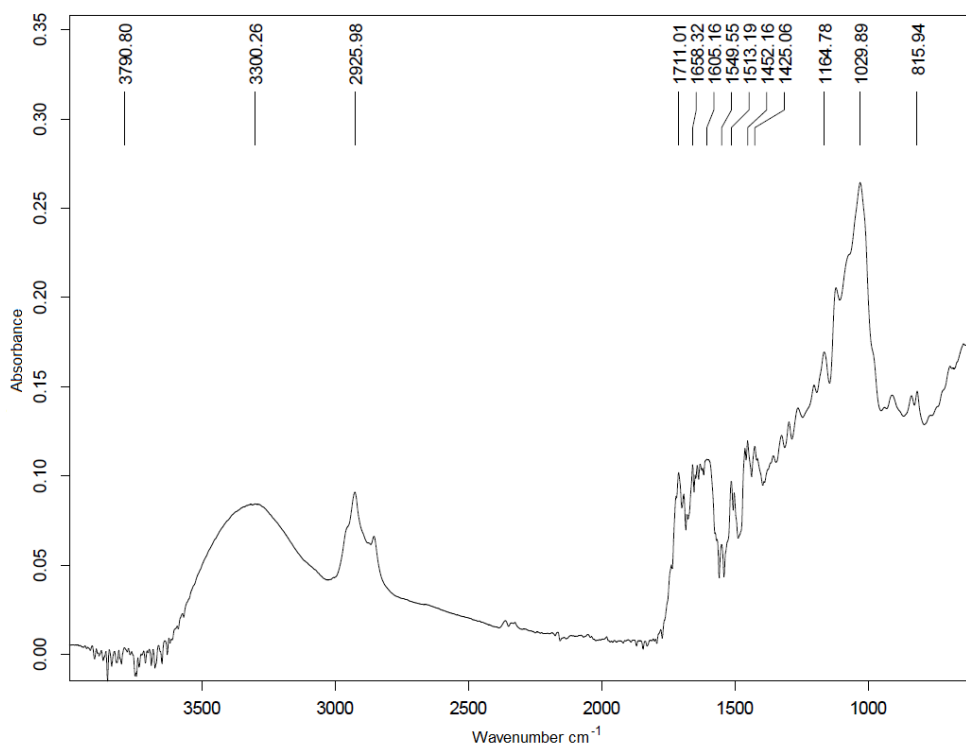


Figure 51. Spectra from FTIR measurement on reaction VIIb at 50°C.

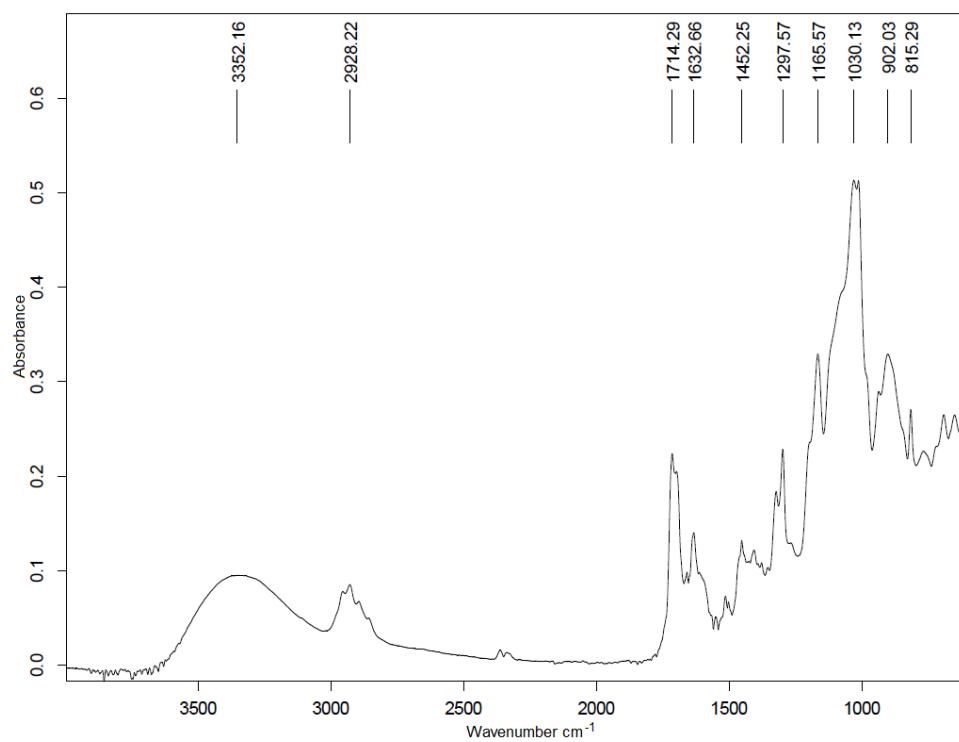


Figure 52. Spectra from FTIR measurement on reaction VIIa at 25°C.

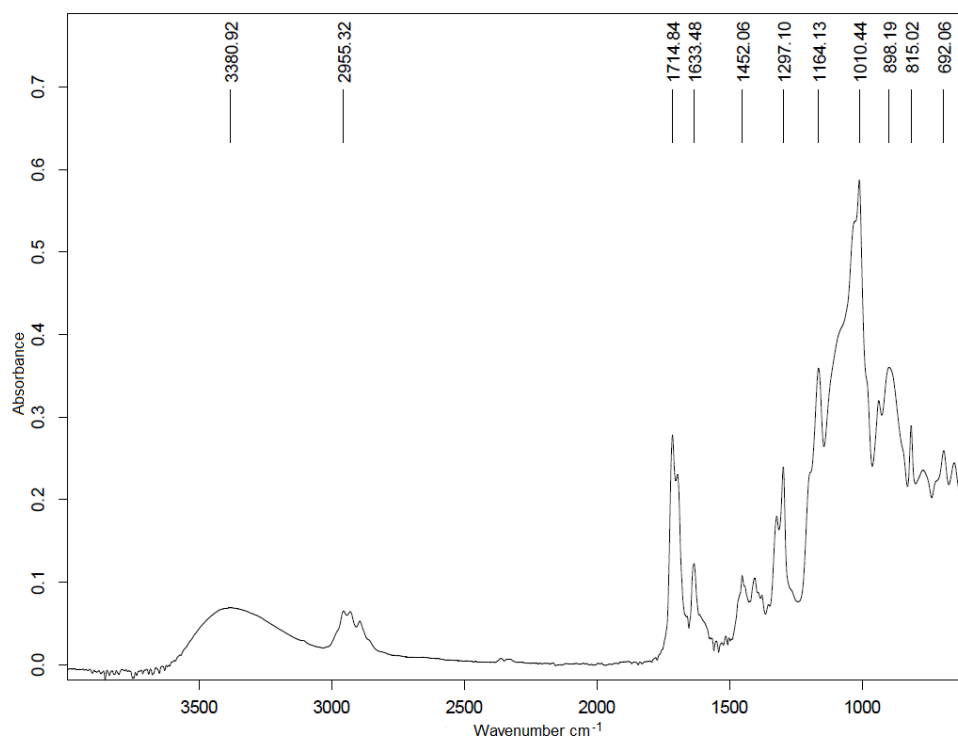


Figure 53. Spectra from FTIR measurement on reaction VIIa at 50°C.

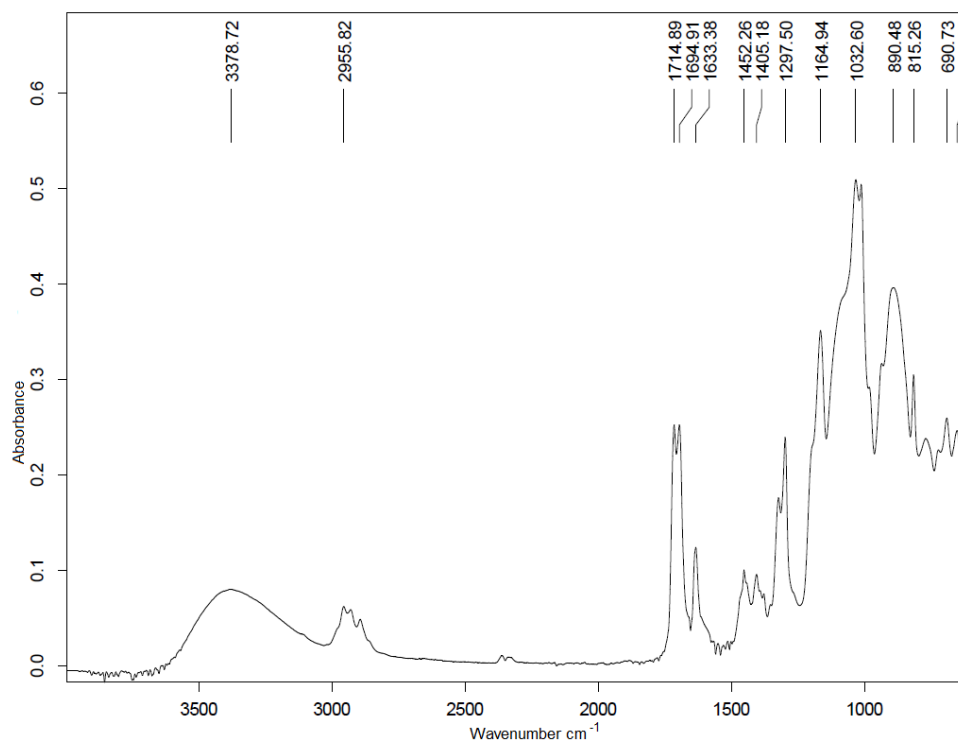


Figure 54. Spectra from FTIR measurement on reaction VIIb at 25°C.

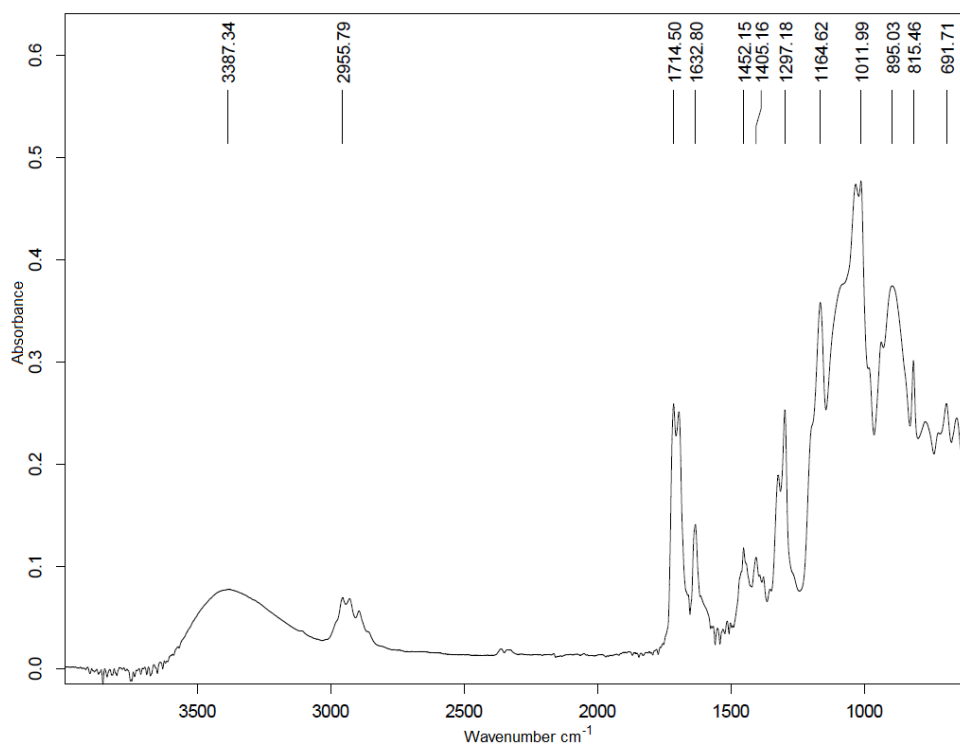


Figure 55. Spectra from FTIR measurement on reaction VIIb at 50°C.

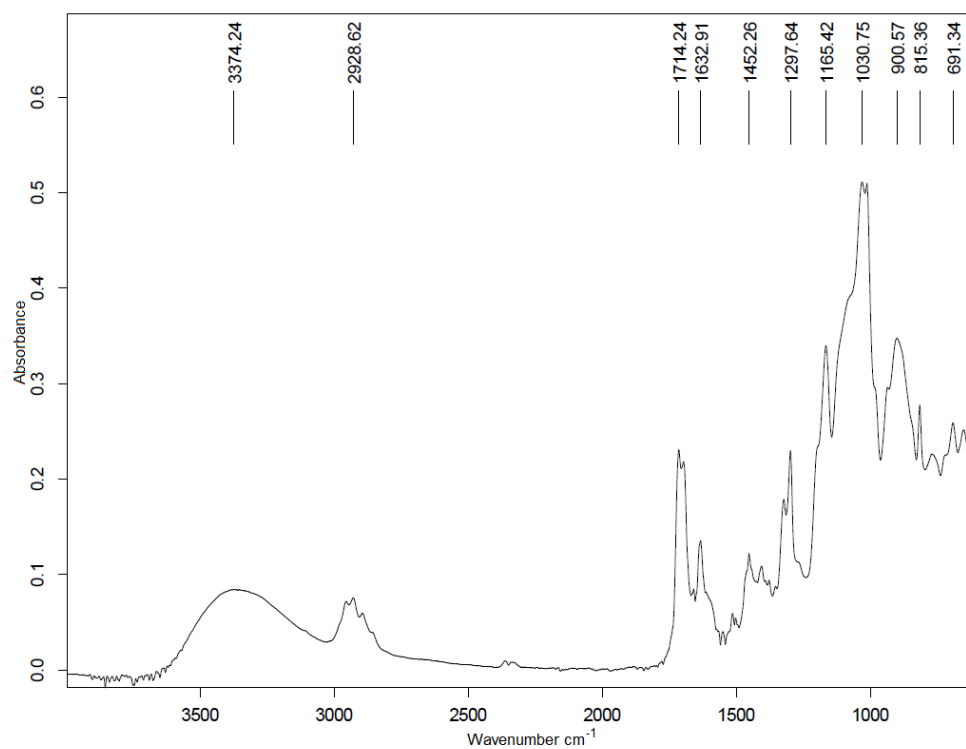


Figure 56. Spectra from FTIR measurement on reaction VIIIa at 25°C.

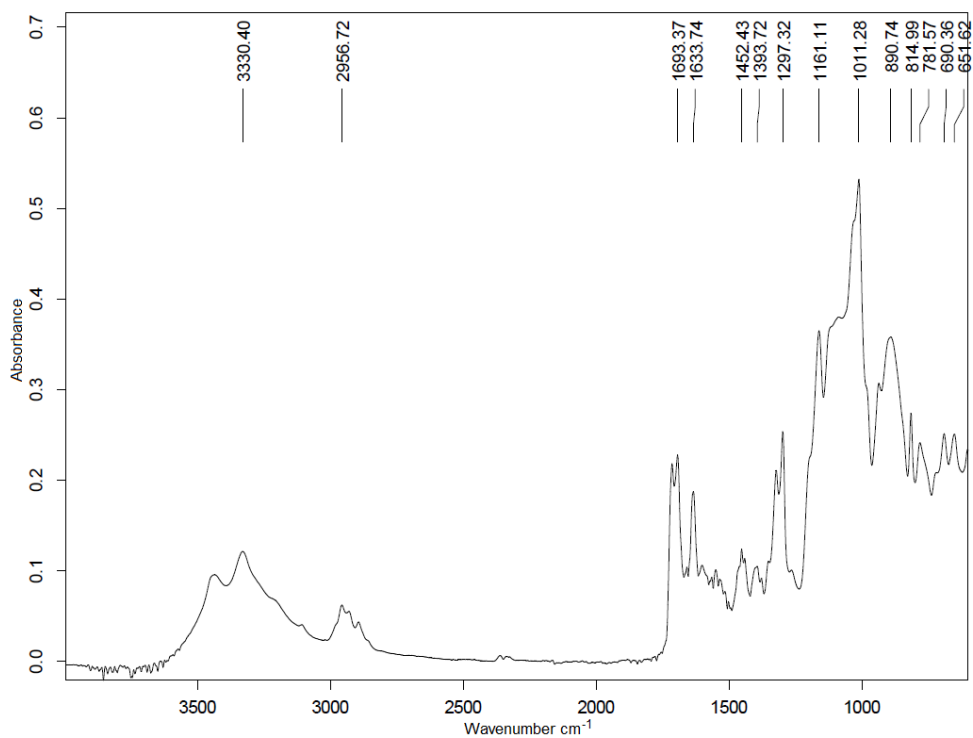


Figure 57. Spectra from FTIR measurement on reaction VIIIa at 50°C.

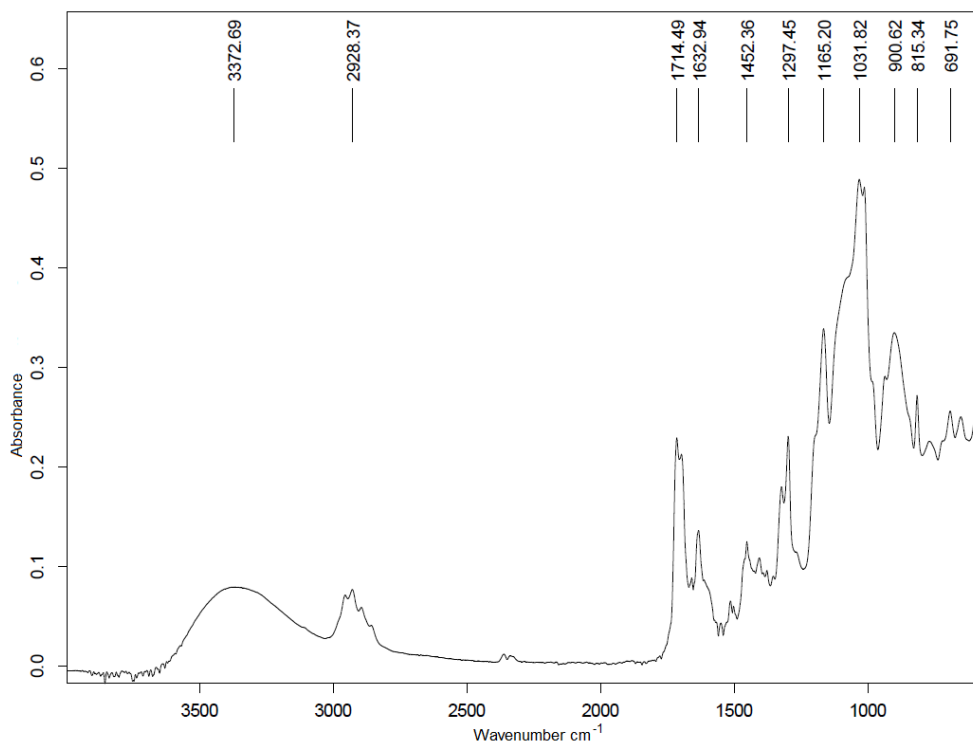


Figure 58. Spectra from FTIR measurement on reaction VIIIb at 25°C.

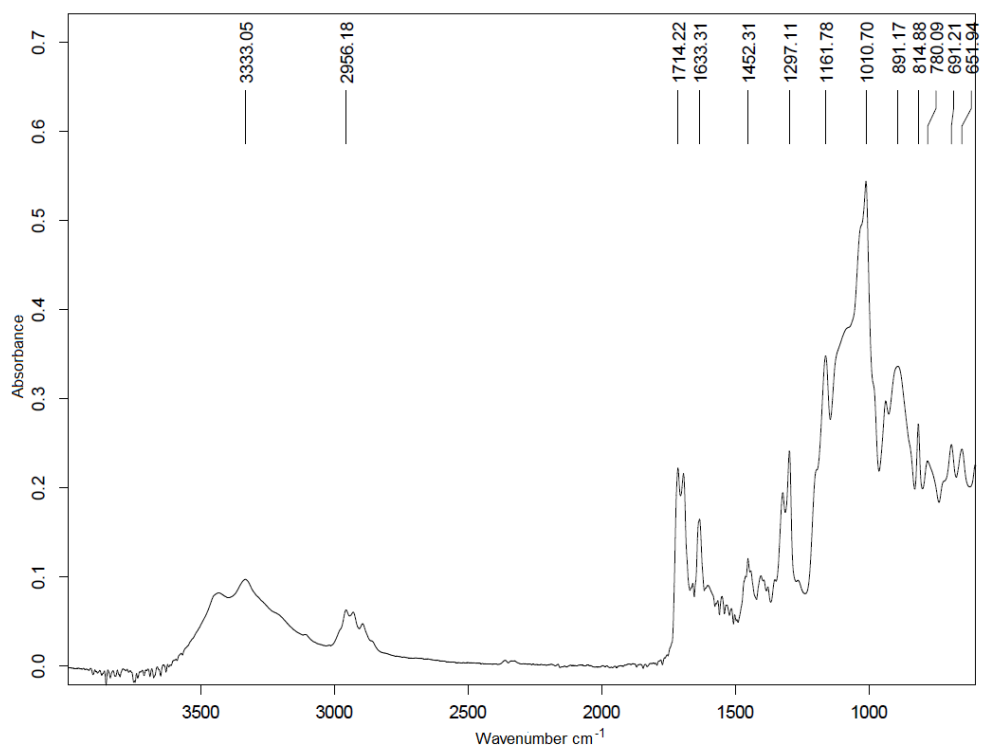


Figure 59. Spectra from FTIR measurement on reaction VIIIb at 50°C.